ADVANCED FUNCTIONAL MATERIALS
www.afm-journal.de

Stimuli-Directing Self-Organized 3D Liquid-Crystalline Nanostructures: From Materials Design to Photonic Applications

*Ling Wang and Quan Li**

3D photonic nanostructures with desirable functionalities in the visible light region and beyond have been recently given vast and increasing attentions because of the ability to control or confine electromagnetic waves in all three dimensions. Although substantial progress has been made in fabricating 3D nanostructures by means of lithography and nanotechnology, various bottlenecks still need to be overcome, and developing soft 3D stimuli-directed nanostructures with tailored properties remains a challenging but exciting work. In this context, soft nanotechnology—i.e., exploiting self-organized soft materials in nanotechnology—is emerging as a vibrant and burgeoning field of research in the bottom-up nanofabrication of intelligent stimuli-driven 3D photonic materials and devices. Liquid-crystalline materials undoubtedly represent such a marvelous dynamic system that combines the liquid-like fluidity and crystal-like ordering from molecular to macroscopic material levels. Importantly, being "soft" makes the materials responsive to various stimuli such as temperature, light, mechanical force, and electric and magnetic fields as well as chemical and electrochemical reactions, resulting in a fascinating tunability of dynamic photonic bandgaps in the 3D nanostructure that provides numerous opportunities in all-optical integrated circuits and next-generation communication systems. Here, the development of 3D photonic nanostructures is reviewed, culminating with perspectives for the future scope and challenges of these emerging soft 3D photonic nanostructures towards device applications.

1. Introduction: From Natural to Synthetic 3D Photonic Nanostructures

3D photonic nanostructures that can manipulate the flow of light or photons in all three dimensions, and potentially beyond, represent a giant leap to the next-generation nanophotonic technology and the integration or upgrade of currently existing optical-electronic materials and devices.[1] Endowing remote and dynamic stimuli-directed controllability to 3D periodic nanostructures with tailored functionality would provide further impetus for the bottom-up fabrication of nanostructured materials and nanophotonic devices.[2] In this regard, nature has created a multitude of appealing 3D nanostructures through evolution and natural selection over billions of years, thus granting us inexhaustible wealth and inspiration. The beetle *Pachyrhynchus argus* from the northeastern part of Queensland in Australia presents a spectacular metallic coloration that is independent of the viewing angle. It has been revealed that the brilliant color may result from a 3D nanostructure analogous to opal nanostructures.[3,4] As is well known, the variation of an opal nanostructure would be the inverse opal that was unexpectedly found in the dorsal wings of some special butterflies (**Figure 1**A,B).[5–7] The complex 3D biophotonic nanostructures in the butterflies are composed of lattices of hollow, air-filled voids within a network of interconnecting cuticle, which could offer excellent reflectivity over a broad angle range. Furthermore, the weevil *Pachyrrhynchus congestus pavonius* demonstrates a vibrant orange color that can be seen in any direction, which is found to be associated with a 3D periodic photonic polycrystal. The long-range disorder introduced by the grain boundaries is thought to result in the shift of the reflection bands to shorter wavelengths with increasing incidence angles, thus providing isotropic scattering along all directions (Figure 1C,D).[8] Interestingly, the sea star *Ophiocoma wendtii* usually changes color from banded gray at night to dark brown during the day, and can respond swiftly to the shadows, thus escaping from predators; this colour change is attributed to the unique 3D mesh nanostructures capable of focusing the incident light from the ambient enviroment (Figure 1E,F).[9–11] All these 3D nanostructures in nature with unique biological and photonic functions provide incredible blueprints toward the design, fabrication and characterization of artificial 3D photonic architectures for various device applications.

Inspired by natural creatures, researchers have recently devoted extensive efforts to fabricating 3D photonic nanostructures with controlled symmetry, size and defects on a large scale. Generally, the fabrication processes are divided

Dr. L. Wang, Prof. Q. Li
Liquid Crystal Institute and Chemical Physics Interdisciplinary Program
Kent State University
Kent, Ohio 44242, United States
E-mail: qli1@kent.edu

DOI: 10.1002/adfm.201502071

into *bottom-up* and *top-down* methods. The *bottom-up* methods are primarily about the self-assembly of component units or building blocks such as emulsions, colloidal particles, and block copolymers.[12–14] Unfortunately, various undesired dislocations or defects are often inevitably introduced in the processes of self-assembly, such as impure phases, missing local particles and uncontrollable molecular orientations. In contrast, *top-down* methods are mostly based on lithography-related techniques including layer-by-layer stacking by the method of soft lithography,[15] and micropositioner-assisted deposition of component solutions,[16] etc. *Top-down* soft lithography provides a fascinating avenue to develop 3D photonic nanostructures without defects. However, lattice distortion often occurs due to the optical refraction and film shrinkage in the processes of lithography; local structrual collapse or cracks are more likely to happen in the 3D superstructures because of thermal and mechanical instabilities during template removal and inescapable backfilling steps. Moreover, there is increasing interest in developing 3D nanostructures from environmentally sensitive soft materials, such as hydrogels, which are sensitive to different stimuli, and infiltration of responsive soft materials into the 3D nanostructured templates.[17–20] However, the research is still in its infancy, and various obstacles need to be overcome before the widespread applications of the 3D photonic crystals could eventually take off.

Keeping pace with the rapid expansion and advancement of nanoscience and nanotechnology, multitudinous soft materials have vigorously stridden into mainstream areas of soft nanophotonics.[21–23] The intrinsic self-organization of these materials has been ingeniously utilized to fabricate a panoply of 3D photonic nanostructures for a diverse range of novel applications. Liquid crystal (LC) materials undoubtedly represent a most engrossing state of matter, combining liquid-like fluidity and crystal-like ordering from molecular to macroscopic material levels.[24–29] Depending on the level of ordering of the LC molecules, diverse and abundant phases have been widely demonstrated: (1) a nematic phase possesing only orientational order where the molecules self-organize along the unique *director*, (2) a smectic phase with both orientational and translational ordering which results in the molecular alignments into layers or planes, and (3) other complex but fantastic liquid-crystalline phases, including chiral nematic or cholesteric phases, cubic blue phase, and so forth.

LC displays (LCDs) based on conventional nematic LCs now dominate the global market of advanced information displays with an annual worth of more than $100 billion, and have drastically revolutionalized the way that information is presented. With LCDs ubiquitous in our daily life, research and applications of LCs are rapidly venturing into the forefront of the bottom-up nanofabrication of advanced photonic materials and devices, and promising new techniques have also been developed to controllably fabricate the liquid-crystalline nanostructures with tailored configurations.[30–32] Different from the conventional photonic nanostructures fabricated by expensive, time-consuming, environmentally hazardous and scale-prohibitive manufacturing procedures of semiconductor-based inorganic nanostructures, the unique self-organization properties inherent in the liquid-crystalline materials make it a quite advantageous approach toward the "green", efficient, and cost-effective production of large-scale 3D periodic nanostructures. Thanks to the high flexibility of the self-assembly processes, unique building blocks and novel tuning mechanisms could be developed depending on the specific applications. Importantly, being "soft" makes the liquid-crystalline materials responsive to various stimuli such as temperature, light, mechanical force, electric and magnetic field, and chemical and electrochemical reaction, resulting in tunable photonic bandgaps in the 3D nanostructure. Compared with traditional 3D photonic crystals, the unrivalled attributes, such as multi-stimuli-responsiveness, easy tunability, and real time reconfigurability, 3D liquid-crystalline photonic superstructures would undoubtedly provide tremendous opportunities in the widespread applications of all-optical integrated circuits and next-generation communication systems.

This review is dedicated in introducing up-to-date significant advancements of the most fascinating themes about stimuli-directing self-organized 3D liquid-crystalline photonic

Ling Wang is currently a postdoctoral research associate in the group of Prof. Quan Li at the Liquid Crystal Institute, Kent State University. He received his Ph.D. from the Department of Materials Physics and Chemistry in University of Science and Technology Beijing (2013), and then worked as a research associate in the Department of Materials Science and Engineering, Peking University together with his advisor Prof. Huai Yang. His current research focuses on the design, synthesis, and applications of liquid crystal materials, stimuli-responsive molecular switches, and novel functional nanomaterials.

Quan Li is Director of Organic Synthesis and Advanced Materials Laboratory at the Liquid Crystal Institute of Kent State University, where he is also Adjunct Professor in the Chemical Physics Interdisciplinary Program. He received his Ph.D. in Organic Chemistry from the Chinese Academy of Sciences (CAS) in Shanghai, where he was promoted to the youngest Full Professor of Organic Chemistry and Medicinal Chemistry in February 1998. His current research interest spans from stimuli-responsive smart soft matter, advanced photonic and optoelectronic materials for energy-harvesting and energy-saving, and functional biocompatible materials and nanoparticles to nanoengineering and device fabrications.

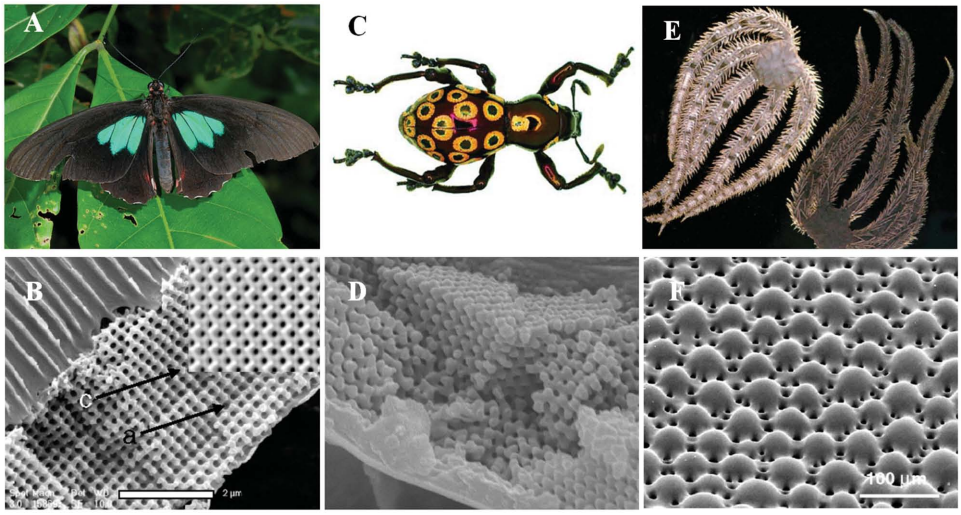

Figure 1. 3D photonic nanostructures in nature. A) Photo of the *P. sesostris* butterflies. B) The nanostructure of their dorsal wings under the scanning electron microscope (SEM). C) Photo of the *Pachyrrhynchus congestus pavonius* weevil. D) SEM of its interior structure. E) The color changes of *Ophiocoma wendtii* brittle stars during the day and night. F) SEM images of the microlens arrays on the surface of one dorsal arm. Reproduced with permission. A) Reproduced with permission.[4] Copyright 2004, Royal Society of Chemistry. B) Reproduced with permission.[7] Copyright 2010, National Academy of Sciences. C,D) Reproduced with permission.[8] Copyright 2007, American Physical Society. E,F) Reproduced with permission.[11] Copyright 2004, Royal Society of Chemistry.

superstructures. We will start with the self-organized LC blue phase 3D cubic nanostructures, where methods of precisely constructing or tuning these self-organized superstructures with different stimuli and their promising applications are discussed. We then introduce the design, fabrication and applications of self-organized 3D liquid crystalline microdroplets and microshells, self-organized 3D topological defects in LC smectic focal conic domains, and self-organized 3D polymeric liquid-crystalline photonic nanostructures. The review concludes with perspectives for the future scope and challenges for these emerging 3D soft nanostructures and their micro/nanophotonics. We hope that this review and further efforts in the field will guide researchers toward cost-effective and highly efficient production of large-scale 3D photonic nanostructures and their real-world widespread applications.

2. Self-Organized Liquid-Crystal Blue Phase 3D Cubic Nanostructures

2.1. Laser Emissions in Blue Phase 3D Cubic Nanostructures

Blue phases (BPs) are among the most fascinating soft photonic nanostructures in the area of LCs. They are known to self-organize into the 3D frustrated nanostructures, which originate from the competition between the packing topology and chiral forces. The periodic nanostructures are self-organized from the so-called double-twisted cylinders that are usually stabilized by the formation of defects or disclinations.[33,34] The defects inevitably occur because the double-twisted structures are unable to continuously fill the 3D space. As a result, the local tendency for stability toward a double-twisted arrangement and the global tendency for stability toward the defect-free space counteract each other. If the former tendency exceeds the latter, BPs are supposed to appear, while the result is a chiral nematic phase if the latter prevails. For this reason, stable BPs often appear in the temperature range close to that of an isotropic phase, in a chiral nematic phase, which has short pitch with larger twisting forces.[35]

Hitherto, three types of BPs have been widely reported and investigated, i.e., BP III (Blue Phase III), BP II (Blue Phase II), and BP I (Blue Phase I), which are suppposed to sequentially appear when cooling a high chirality liquid crystalline mixture from the isotropic state to cholesteric phase.[36–42] It has been theoretically and experimentally verified that the BP III is naturally amorphous, while the BP II and BP I present in the form of simple cubic (SC) and body-centered cubic (BCC) nanostructures, respectively. The periodicity and reflection wavelength of BP I and BP II are typically in the spectral range of visible light, and therefore BPs have been widely considered as one of the highly promising candidates for self-organized 3D photonic crystals.[43] The reflection peaks usually appear at (110), (200), (211), etc. in BP I, and (100), (110), etc. in BP II. These reflections satisfy the following equation:[44]

$$\lambda = \frac{2na}{\sqrt{h^2 + k^2 + l^2}}$$

where λ, n, and a denote the wavelength of incidence, refractive index, and lattice constant, respectively; and h, k, and l are the Miller indices. The value of $h + k + l$ is an even number in BP I, and an odd number in BP II. In typical BPs, the bandgap photonic reflections are usually generated by the light diffracted from the (110) and (200) directions of BP I and the (100) direction of BP II. These reflection wavelengths usually appear in the visible region.

Interestingly, laser emissions in three orthogonal directions have been detected simultaneously in the 3D photonic BP II.[45,46] As shown in **Figure 2**, BP II soft crystals are typically stacked by the double-twisted cylinders in three dimensions

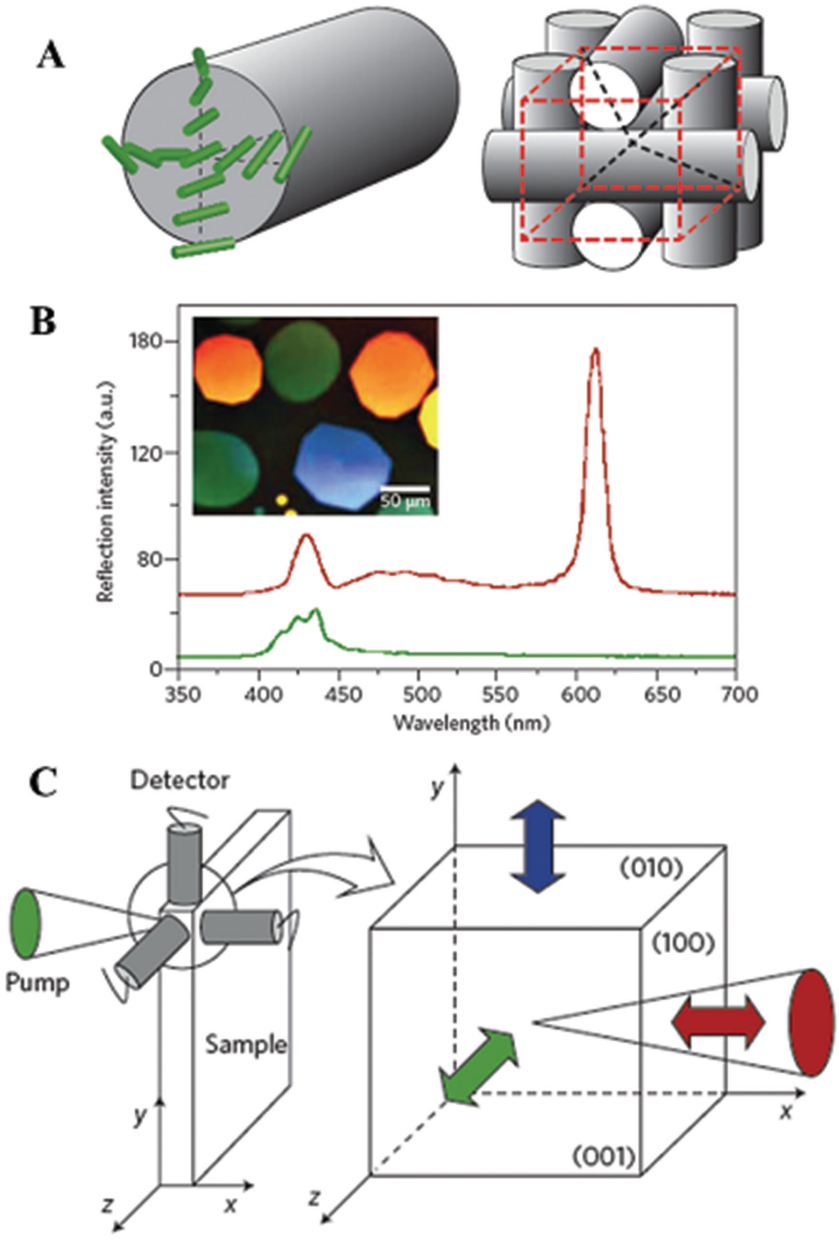

Figure 2. Laser emissions in three orthogonal dimensions from the BP II cubic superstructures. A) Schematic illustration of the double-twist structure and the resultant simple cubic BP II. B) Reflection spectra of BPII single crystals (red) and cholesteric phase (green); the inset shows the typical POM textures of BP II. C) Regions of the sample from which the laser emissions can be detected in three orthogonal directions. Reproduced with permission.[45] Copyright 2002, Nature Publishing Group.

with cubic symmetry, which is somewhat similar to the scaffold and wood-pile structures.[47,48] The colorful red, green and blue textures under the polarizing optical microscopy (POM) with crossed polarizers arose from the Brag reflection of different lattice planes, e.g., (100), (110), etc. When one of the platelet BP domains in a LC thin cell is excited by the pump laser beam, laser emissions in the orthogonal (100), (010) and (001) directions can be observed at the same time, which is actually a sign of the distributed feedback in three dimensions. Subsequently, laser emissions have also been demonstrated in both the polymer-stabilized BP I and other low-molecular-weight LCs with wide temperature BP ranges, which undoubtedly pave a significant avenue for the practical photonic applications of BPs.[49,50] Moreover, Chen et al. recently demonstrated the coherent random laser emissions in the dye-doped cubic BPs,[51] where the optical feedbacks came from the interferences and recurrent multiple scattering around the grain boundaries of BP polycrystal. It is noteworthy that the threshold energy of laser excitation in BPs was observed to be much lower than that of the corresponding chiral nematic or cholesteric LCs, and these elegant soft 3D photonic materials should also find widespread applications in sensing, switching, waveguiding, etc.

2.2. Stimuli-Directed Liquid Crystal Blue Phase 3D Cubic Nanostructures

As the soft 3D photonic crystals, BPs feature remarkable bandgap tunability over an extensive spectrum in response to various external stimuli. The spectral bandgap position of selective reflection can be readily predetermined by varying the chiral fraction of BP mixtures.[52] Given the thermotropic nature of the liquid-crystalline BP hosts, it is unsurprising that all the 3D cubic nanostructures are thermally sensitive, but the shift of reflection wavelength is usually quite narrow, typically <50 nm. Choi et al. recently reported the BPs with widely tunable wavelength by incorporating an unusual bent-core mesogen into commercially available multicomponent rod-like nematogen mixtures.[53] As shown in **Figure 3**, the colors of platelet textures observed under the POM with crossed polarizers are found to gradually shift toward a longer wavelength when decreasing the temperature, where the corresponding reflection presumably arose from the Bragg-reflection effect in the (200) plane of the body-centered-cubic lattices. A large shifting of ≈150 nm in the reflection wavelength was achieved with a temperature change of ≈25 °C, which might result from the stabilization of BPs and the unique temperature-sensitive properties of unusual bentcore mesogen.[54] To realize BPs with much wider tuning wavelength from ultraviolet to visible and even infrared regions, one of the promising methods should be the development of unprecedented chiral molecular switches which exhibit high helical twisting powers and large variations with temperature changes. The manifestation of thermally induced color changes should find many emerging applications for broad civilian and military devices.

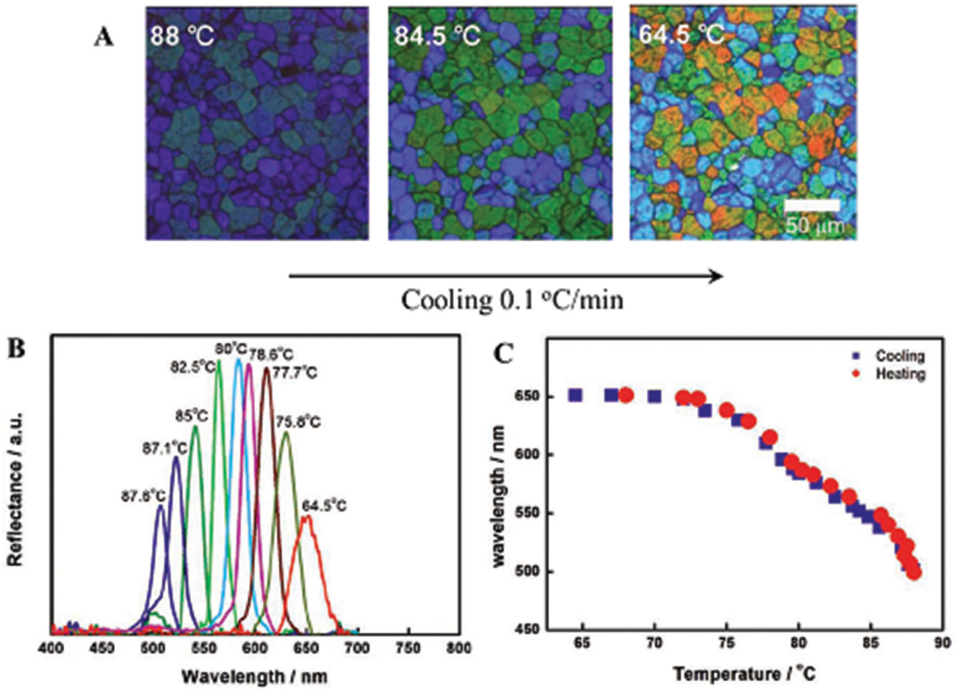

Figure 3. Thermally directed BP 3D cubic nanostructures. A) Typical POM images during the cooling process. B) Temperature-dependent reflection spectra. C) Change of the central wavelength during cooling and heating processes. Reproduced with permission.[53]

Applying a pressure stimulus to the BP materials is somewhat equivalent to the control over their density, therefore the resulting behaviors should be similar to the corrresponding thermal counterpart in phase sequence and photonic bandgap shifting.[55] In terms of mechanically directed bandgap tuning, Castles et al. recently demonstrated color tuning in selective reflection by stretching a free-standing BP gel, where the interplanar spacing along the surface normal would be condensed under lateral stretch, and eventually leading to a blue-shifted reflection color.[56] This kind of self-organized 3D photonic crystals was fabricated by an in situ photopolymerization of the mixtures with polymerizable liquid-crystalline monomer and di-acrylate reactive mesogens. After photopolymerization with ultraviolet irradiation, the BP film appeared macroscopically as solids at room temperature, where the corresponding structure of liquid-crystalline phase was confirmed as that of body-centered-cubic BP I based on the standard techniques including optical Kossel diffraction analysis, polarizing optical microscopy and spectral analysis. Upon stretching, a color change in the spectral ranges of visible light was apparently observed across the liquid-crystalline gel films as shown in **Figure 4**. When a lateral stretch was applied, the thickness of BP film

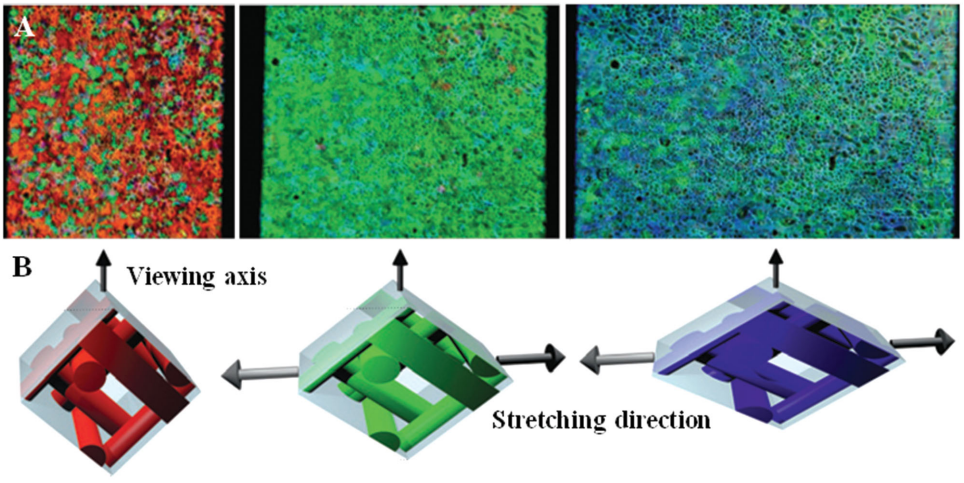

Figure 4. Color changes in a stretchable BP 3D cubic nanostructure. A) Optical textures of a BP film upon stretching under the polarizing optical microscope with crossed polarizers. B) Schematic illustration of the possible deformation of the body-centered-cubic BP I lattices. Reproduced with permission.[56]

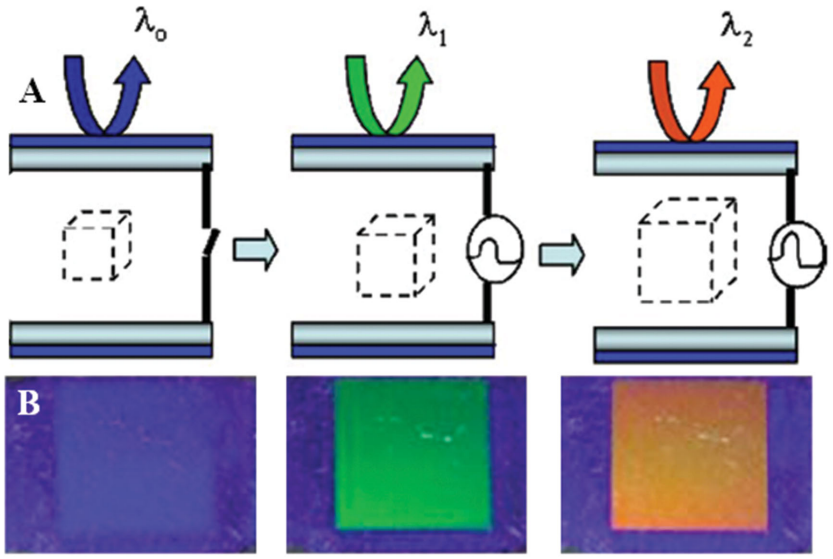

Figure 5. Electrostrictions in a polymer-stabilized BP 3D cubic nanostructure**.** A) Schematic illustration of the cubic lattice distortion with an increase in applied voltage. B) Corresponding photographs of the Bragg reflection under different voltages, 0 V (blue), 33 V (green), and 40 V (red). Reproduced with permission.[62] Copyright 2010, Optical Society of America.

was reduced while a mechanically induced chromic behaviour was observed due to the contraction of the effective lattice periodicity in the viewing direction. This kind of optical effect was somewhat analogous in many ways to the one-dimensional photonic bandgaps in the reported chiral nematic or cholesteric elastomers.[57] Morever, a novel Pockels electro-optical effect under the alternating current electric field was unexpectedly discovered in the mechanically deformed cubic BP nanostructures, which is expected to provide new theoretical inspirations or concepts for developing the unprecedented electro-optic devices with ultra-low driving voltage.

The most complicated but extremely useful way of controlling the selective reflection would be to apply an electric field. BPs are known to exhibit three distinct transformations upon applying an electric field: local director reorientation, lattice distortion (i.e., electrostriction) and field-induced phase transitions.[58] The local director reorientation, so-called Kerr effect, is actually the fundamental principle for next-generation ultrafast liquid crystal displays which is known for submillisecond-scale switching speed.[59] Generally, electrostriction and field-induced phase transitions occur when a strong electric field is applied in BPs, which often leads to beautiful color shifts of the selective reflection. The response speed in these cases is much slower than that of Kerr effect, which could be attributed to the movement and rearrangement of 3D disclinations within the lattices.[60,61] Compared to the electrostrictions, field-induced phase transitions need much higher field strength and usually result in a discontinuous and irreversible shifts of photonic bandgaps. It is noteworthy that Lu et al. reported a full visible color switching of reflection wavelength in the polymer stabilized cubic nanostructures.[62] The distortion of cubic BP lattices under the applied field resulted in the reflection color change from blue, green to red as shown in **Figure 5**, where the introduction of a small amount of polymer network in cubic BPs was believed to stabilize against the occurrence of field-induced phase transitions and broaden the range of electrically switchable color in the visible spectrum.

Among various promising stimuli, light shows distinct and significant advantages due to its spatial, remote, and temporal controllability in different external environments. It is also noteworthy that the light sources with different wavelength, intensity and polarization are readily accessible. Light-driven self-organized blue phase 3D cubic nanostructures have received increasing attentions especially in recent years, but the reflection wavelength tuning is usually quite narrow.[63–65] The ability to dynamically tune the photonic bandgap in cubic BPs across a wide wavelength range is highly desirable, but it has not been realized due to various obstacles including the instability and irreversibility of BPs under the light irradiations. Li et al. recently made a breakthrough of full visible range reflection phototuning in cubic BPs by using an axially chiral azobenzene molecular switch as shown in **Figure 6**A.[66] It is a timely and significant progress in areas of reversible phototunable red, green, and blue (RGB) reflections, i.e., bridging the visible, in self-organized 3D photonic nanostructures.[67] As illustrated in Figure 6B and 6C, a red-shift in photonic bandgap reflection occurred upon the irradiation of 408 nm light, which presumably arose from the decrease in the chirality of the molecular switch doped in the BPs. Interestingly, the simple cubic BP II was found to transform toward the highly ordered body-centered cubic BP I phase during the light irradiation process, and the reverse process occurred under 532 nm light irradiation. All the above structural transformations have been thoroughly indexed and confirmed using a optical Kossel diffraction diagram. As shown in Figure 6D, the circle patterns of the (100) lattice of BP II enlarged, switched to diamond-shaped pattern corresponding to (110) lattice of BP I, and gradually shrinked when the irradiationg time increased from 0 to 15 s. Such self-organized liquid-crystalline nanostructures undoubtedly provide an attractive impetus for developing the optically tunable soft 3D photonic crystals for next-generation all-optical device applications.

However, exploiting the high-energy ultraviolet light in the liquid-crystalline material systems may sometimes lead to component degradation or damage, photochemical contamination, as well as poor penetration through the samples, and so forth. Utilizing near infrared (NIR) irradiation is supposed to be much preferred in areas of life sciences, materials science, and aerospace applications of photoresponsive systems owing to its distinct invisibility and superior penetration for spatially and temporally remote activation.[68–71] Recently, Li et al. demonstrated that a NIR light-sensitive self-organized 3D photonic superstructure could be fabricated by doping novel surface-functionized plasmonic gold nanorods into a liquid-crystalline BP host as shown in **Figure 7**.[72] The resultant 3D photonic nanostructures could be switched between simple cubic (BP II)

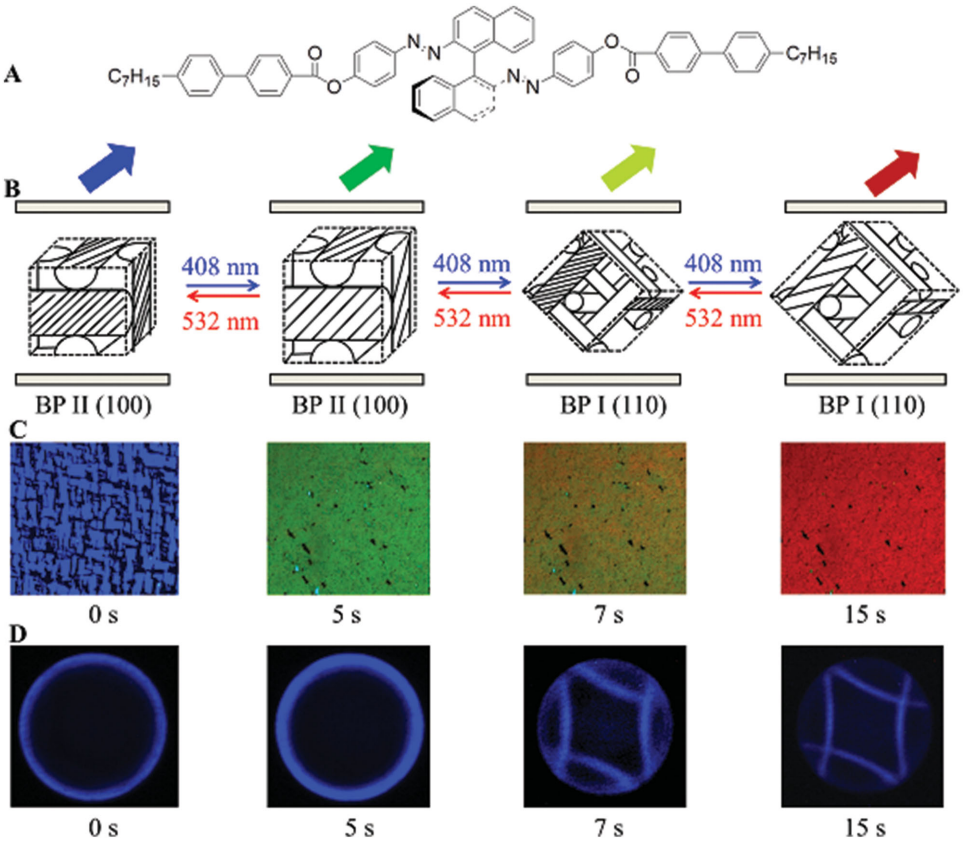

Figure 6. Phototunable self-organized blue phase 3D cubic nanostructure**.** A) Molecular structure of light-driven chiral switch. B) Schematic illustration of BP cubic nanostructures. C) Reflection color images of BPs upon 408 nm light irradiation. D) The corresponding optical Kossel diffraction diagrams. Reproduced with permission.[66]

and body-centered cubic (BP I) symmetry under the irradiation of a NIR laser, which results from the significant photothermal surface plasmonic resonance effect from the embeded gold nanorods. The reverse process occurs upon removal of the NIR light irradiation. Furthermore, reversibly dynamic NIR-light-directed reflections over a wide range of wavelengths from such

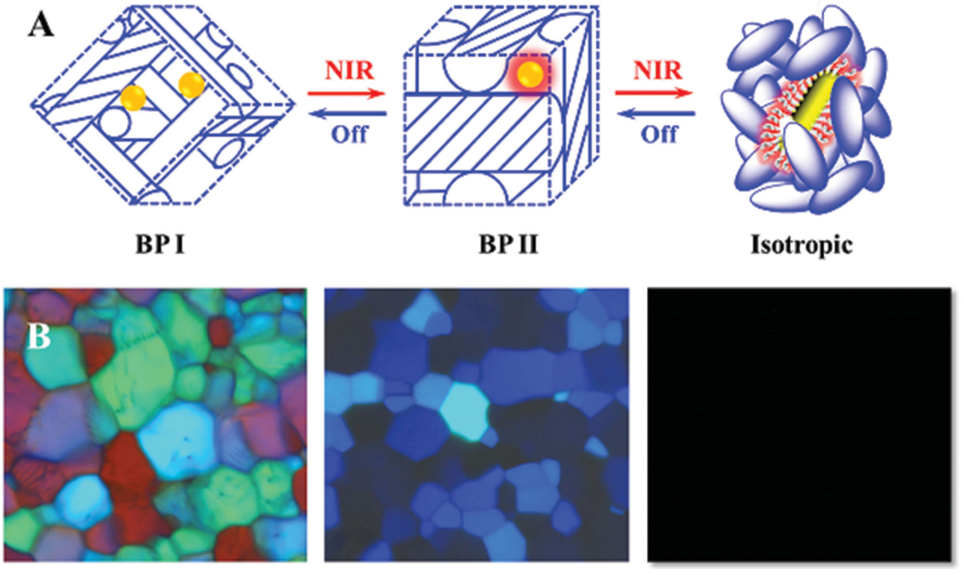

Figure 7. NIR-light-directed self-organized BP 3D photonic superstructures. A) Schematic illustration of the structural transformations under the NIR-light irradiation. B) Typical optical textures of BP I and BP II nanostructures.

3D soft photonic crystals were obtained. The research could provide a versatile approach to temporally and spatially manipulate the 3D self-organized nanostructures and their dynamic photonic properties, which might lead to the emerging device applications of such 3D photonic crystals for next-generation of optical communication technology.

It should be pointed out that developing the chemically responsive BP photonic superstructures for sensitive chemical sensors remains a less explored but exciting arena. One of the major obstacles in fabricating such 3D sensors may be the narrow temperature range of BPs and the exacting requirements for the liquid-crystalline molecular structures. The recent advancement in developing the stable BP materials with broad temperature ranges and the maturity of next-generation ultrafast BP display should bring an unprecedented golden opportunity for the researchers in this area.[73–75] Similar to the strategy for developing the cholesteric or chiral nematic sensors, we can fabricate the BP sensors responsive to various chemical and electrochemical stimuli in the future research. For example, gaseous carbon dioxide and oxygen monitors based on unique chiral dopants,[76] humidity sensors derived from bis-(binaphthylenedioxy)silane compounds,[77] pH sensors using hydrazone-based switches,[78] and among others.[79–83] Developing these 3D sensors holds an exciting bright future and great potential for implementation in various emerging fields, including environmental monitoring, point-of-care clinical diagnostics, hazard identification or threat detection, etc.[84,85]

2.3. 3D Templates from Self-Organized Blue Phase 3D Cubic Nanostructures

Besides being remarkable dynamic soft materials, BPs are significantly promising for templating the self-assembly of colloidal particles or polymers due to the existence of the intrinsic 3D disclination networks (**Figure 8**A,B), which is expected to open a fascinating research direction for developing complex 3D optical nanostructures that hold tremendous potential for photonic and plasmonic applications.[86–88] Ravnik et al. reported the possible fabrication of 3D colloidal crystals by dispersing various nanoparticles with different sizes into liquid-crystalline BPs (Figure 8C),[89] in which the self-organized topological defect cores of soft cubic nanostructures provide perfect 3D templates for trapping the dispersed colloidal nanoparticles. It was found that the self-organized configuration of nanoparticles depends considerably on the orientational order of the liquid-crystalline molecules, where the self-assembly of nanoparticles and the resultant 3D configurations are greatly influenced by both surface anchoring and the size of nanoparticles. In future research, exploring the interplay between the topological defects of cubic BPs and colloidal nanoparticles might lay down the foundation for developing 3D photonic crystals and even some novel metamaterials.[90]

Recently, Coles et al. demonstrated another versatile approach for the fabrication of photonic polymer materials with self-organized 3D nanostructures by the transfer of BP cubic superstructures to polymer networks (Figure 8D).[91] The BP precursor with photopolymerizable monomers was firstly cured under the ultraviolet light irradiation, and the remaining non-polymerized low-molecular-weight LCs were then removed to generate a 3D template of porous free-standing film retaining the 3D nanostructure of chiral BPs. By refilling the template with an achiral nematic LCs, they successfully fabricated the templated-BPs that hold outstanding thermal stability. This kind of templated-BPs can work as both switchable mirrorless lasers and electro-optical devices. In the future work, such polymer may also be further exploited for templating inorganic materials, and refilling the BP-template with a high-refractive index or semiconductor materials might lead to unexpected optical or electronic properties. Besides that, future research on the dispersion of one- and two-dimensional nanostructures such as nanorods, nanotubes, and graphene derivatives in the above self-organized nanostructures should enable the fabrication of even more complex 3D colloidal nanostructures for applications in micro/nanophotonics and other distinct areas, which would also be an ideal platform to control, explore and understand the organization properties of different nanomaterials from the nanometer to micrometer scales in a controllable and programmable technique.

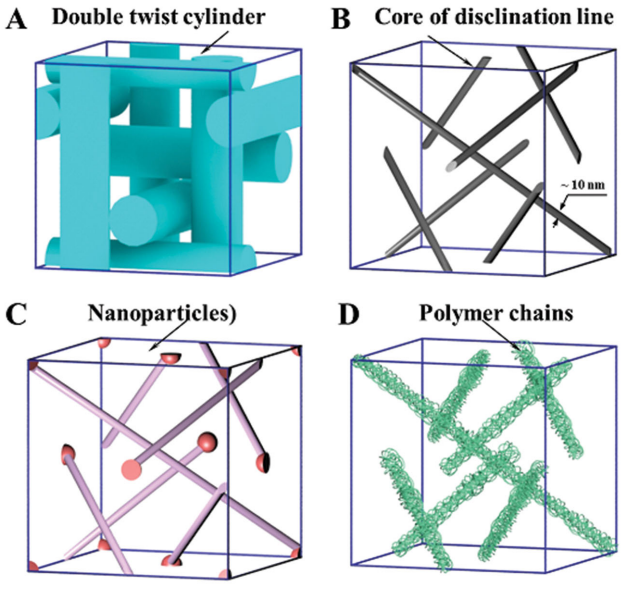

Figure 8. Formation of 3D nanostructures in the BP I template. A) The arrangement of double twist cylinders in a body-centered-cubic nanostructure. B) 3D disclination network in BP I. C,D) Possible aggregations of the nanoparticles or polymers in the 3D BP nanostructures.

3. Self-Organized 3D Liquid-Crystalline Microdroplets and Microshells

3.1. Liquid-Crystalline Microdroplets and Microshells

Self-organized 3D superstructures with spherical configurations have recently received considerable attentions in the forefront of multitudinous research areas, such as optical manipulations, soft photonics, and microfluidics.[92,93] Liquid-crystalline microdroplets and microshells represent an elegant example of the topic. Confining LCs in micrometer or

nanometer-sized systems endows a multitude of thermodynamically stable supramolecular configurations with rich defect topologies. The particular defect configuration or structure lies mainly on the elastic properties of the LCs, the anchoring of the director at the corresponding surface, the size of the droplets or shells, or the presence of external fields.[94–96] Regarding the type of liquid-crystalline materials applied for the microdroplets or microshells and the corresponding type of optical modes, they are basically divided into *nematic* and *cholesteric* microdroplets or microshells.[97,98] The effective and efficient methods to generate the microdroplets are diverse, e.g., dispersion polymerization, induced-phase separation, homogenization, microfluidics, and sonication.[99–103] However, the facile fabrication of liquid-crystalline microshells with controlable sizes over wide range of length scale, stability and multi-dimension organization remains a challenging task. The research and development of LC-related microdroplets and microshells have prosperously evolved into various applications including lasers, displays, biosensors, nonlinear optics, switchable windows, and micro/nanophotonics.[104–107] Herein, we mainly introduce the recent progress toward the design and fabrication of self-organized LC microdroplets and microshells for some novel photonic applications such as optical microresonators, microcavities, and omnidirectional 3D lasing.

3.2. Self-Organized 3D Nematic Liquid-Crystalline Microdroplets

Polymer dispersions of nematic liquid-crystalline microdroplets, i.e., polymer dispersed LCs (PDLCs), have been extensively investigated in the past few years.[108] In the case of PDLCs, the microdroplets are usually made by the phase separation method, where the microdroplets in PDLCs are very dense and of irregular shapes, making it extremely difficult for us to study the optical or photonic properties of individual microdroplets. Recently, Muševič et al. successfully fabricated the microdroplets with a diameter of ≈10 μm by mixing a small amount of dye-doped nematic LCs in polydimethylsiloxane solutions. Interestingly, the resultant nematic liquid-crystalline microdroplets were found to be able to confine the light travelling along the internal surface of the microsphere, and thus can be regarded as a tunable and low-loss whispering-gallery-mode (WGM) microresonator.[109] Compared to the conventional solid-state resonators,[110,111] liquid-crystalline materials systems hold multitudinous advantages such as multistimuli-responsiveness, large tuning range and high Q-factors, and great potential for novel photonic applications including active filters, laser sources, and all-optical switches.

As shown in **Figure 9**A, a uniaxial cross can be observed in the self-organized nematic microdroplets under polarizing optical microscopy with crossed polarizers, from which we can clearly infer that the molecular orientation of LCs inside the spherical cavity is radial. When irradiating one spot of the dye-doped nematic liquid-crystalline microdroplets near the edge with a 514 nm laser source, another bright spot unexpectedly appeared on the other side of the microdroplet. This kind of interesting observation is actually a sign of WGMs in the nematic microdroplets as shown in Figure 9B,C. Upon applying different electric fields, the nematic director orientation inside the microdroplets can be readily modulated, therefore resulting in the tunability of WGMs with a very low external electric field. It is worth mentioning that the electric-field tunability is completely reversible and the tuning range is two orders of magnitude larger than that of conventional

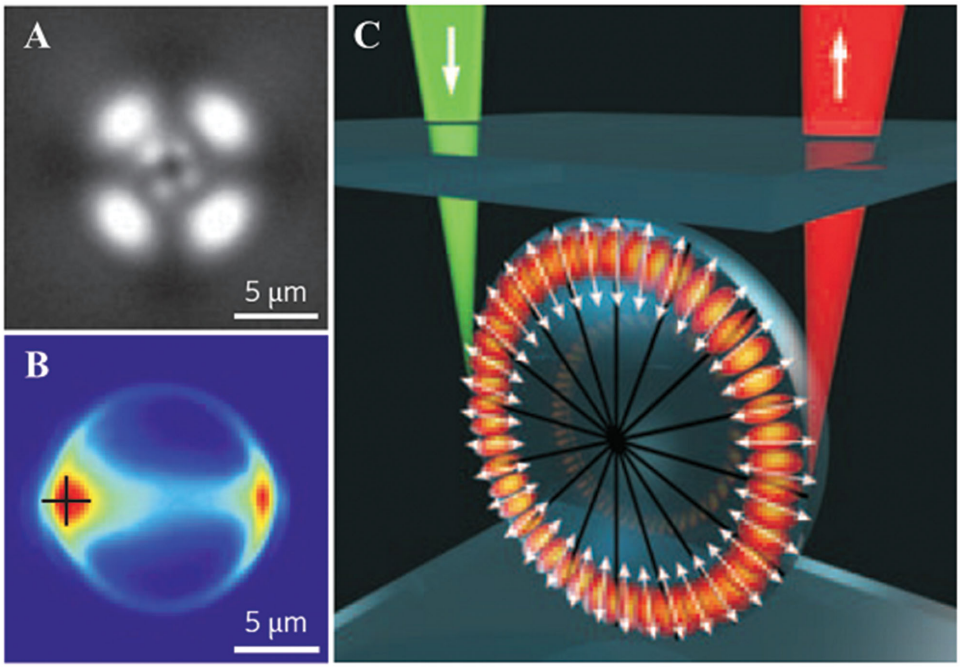

Figure 9. 3D nematic microdroplets as WGM-microresonators. A) Microdroplet of nematic LCs under crossed polarizers. B) Detected light intensity under illumination by a strongly focused laser beam, illuminating the spot (indicated by the black cross) near the edge of the nematic microdroplet. C) Schematic illustration of WGMs in the nematic microdroplet. Reproduced with permission.[109] Copyright 2009, Nature Publishing Group.

solid-state microresonators.[112] In addition, the WGMs in the nematic liquid crystalline microdroplets were successfully tuned by temperature,[113] where the refractive index of LCs is highly temperature dependent and the tunability for the microdroplets is approximately 15 nm for temperature change of 30 K. Subsequently, the WGMs in the self-organized nematic microdroplets have also been tuned by mechanical deformation and chemical reactions.[114] This kind of self-organized liquid-crystalline microdroplets potentially working as microcavities undoubtedly provides a fabulous platform for light manipulation in areas of tunable microcavity lasers, stimuli-sensitive sensors, stimuli-tunable optical microdevices, soft matter photonic circuits, etc.

3.3. Self-Organized 3D Cholesteric Liquid-Crystalline Microdroplets

Bragg-reflector microcavities with spherical configurations, which are usually composed of the alternating concentric shells with different refractive-index materials, are currently a vibrant field of research with an exciting future because of their perfect rotational symmetry in all three dimensions and the ability to confine the light in all optical directions.[115–118] However, it's rather difficult and challenging work to successfully generate the 3D solid-state microcavity.[119] Extensive efforts have been devoted to developing Bragg-onion 3D microresonators in the solid-state nanostructures by the time-consuming chemical synthesis or chemical vapor deposition.[120] Muševič et al. firstly developed the "soft" 3D Bragg-onion microlasers by creating the novel cholesteric liquid-crystalline microdroplets,[121] where the surface tension enabled the LC molecules to spontaneously self-organize into the spherical shape in an immiscible glycerol fluid and the introduction of chirality in cholesteric LCs (CLCs) resulted in the formation of a multilayered spherical Bragg resonator with an alternating periodic refractive-index.

As shown in **Figure 10**A,B, the alternating concentric shells were clearly observed in the cholesteric microdroplets which presumably arose from the radial changes of the refraction index. The period of shells, corresponding to one half of liquid-crystalline pitch, can be readily tuned by using the chiral molecular switches with different helical twisting power or changing their concentration in liquid-crystalline hosts. Within the self-organized cholesteric microdroplets, the helical axis is pointing from the core in all directions to the surface, thus they can work as a spherical Bragg onion microcavity that confines light into the center of the microdroplets. This microresonator can be thought of as hundreds of concentric shells of alternating refractive index as shown in Figure 10C. When doping a fluorescent dye in the CLC host and irradiating the microdroplets with an external pulsed laser, a bright red laser spot unexpectedly appeared in the center of the microdroplets (Figure 10E). The emission intensity was greatly enhanced if the pump laser power was further increased. Interestingly, the laser emissions were independant of viewing directions and can function as a point-like coherent light source, i.e., 3D microlaser. Moreover, the laser emission wavelength depends exclusively on the intrinsic helical pitch of CLCs that could be widely tuned by various external stimuli. The reported procedure of creating the 3D cholesteric microlaser by mechanical mixing method is straightforward, and can quickly and efficiently produce billions of cholesteric microdroplets. However, the wide size-polydispersity of microdroplets thus prepared is always a challenging issue that must be solved toward the widespread applications for soft-matter photonic devices and other areas.

Thanks to the recent advances of microfluidic techniques, we can readily fabricate stable 3D monodisperse cholesteric microdroplets with controllable symmetry, shapes and sizes.[122]

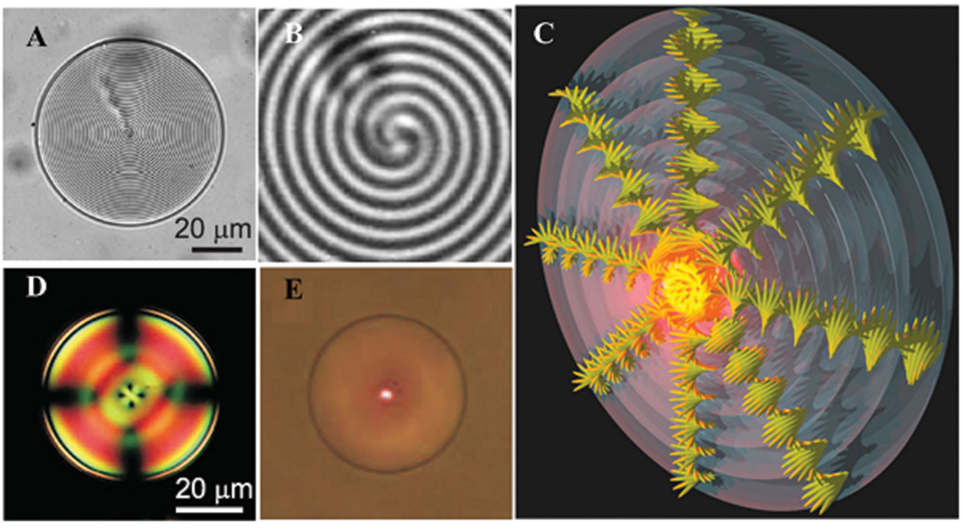

Figure 10. 3D Bragg-onion cholesteric microlaser. A) The cholesteric microdroplet in glycerol. B) Magnification of the central part of a microdroplet. C) Schematic illustration of the liquid crystalline molecular arrangement in one microdroplet. D) A cholesteric microdroplet under the polarizing optical microscopy with crossed polarizer. E) 3D omnidirectional laser emissions in a cholesteric microdroplet. Reproduced with permission.[121] Copyright 2010, Optical Society of America.

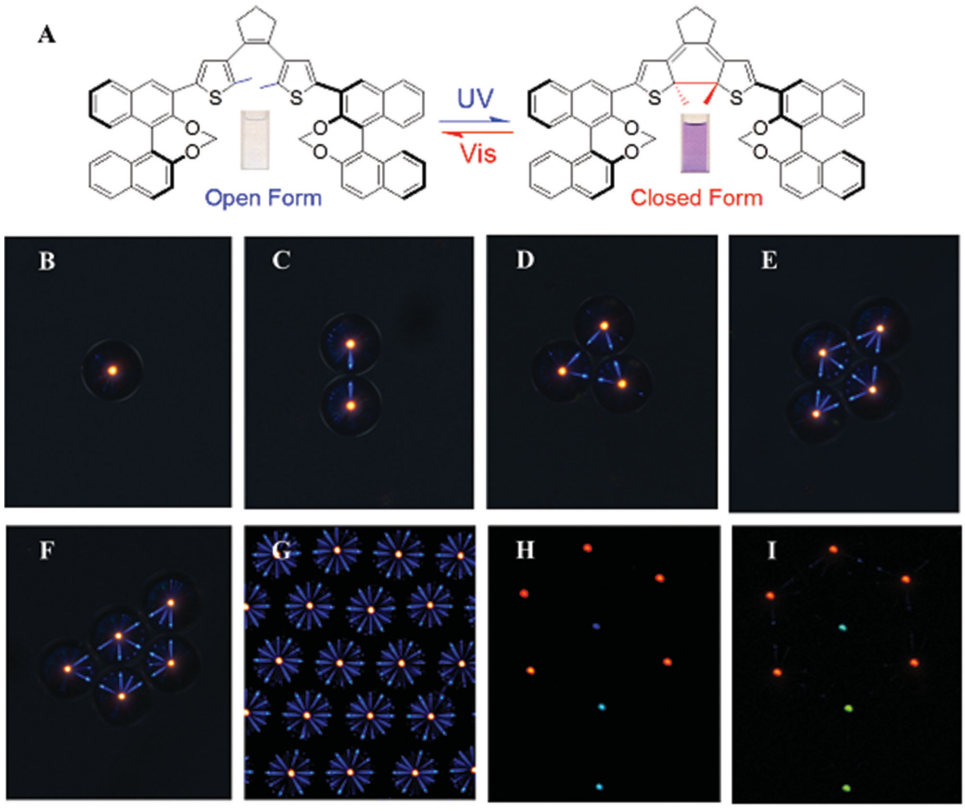

Figure 11. Photonic communication in the monodisperse 3D cholesteric microdroplets. A) Molecular structure of light-driven chiral switch. B–G) Polarizing optical microscopy images and photonic cross-communication of linear-, triangular-, and diamond-shaped patterns in the cholesteric microdroplet arrays. H,I) The "flower-opening" patterns of microdroplets with light-driven iridescent colors. Reproduced with permission.[123]

Moreover, the microfluidic techniques have also successfully overcome the size-polydispersity obstacles during the processes of producing the microdroplets, thus opening infinite possibilities for emerging applications in areas of advanced photonic materials and devices. Recently, Li et al. demonstrated the photonic cross-communication between CLC monodisperse microdroplets, where their self-assembly was precisely manipulated by using the microfluidic method.[123] Only a central reflection spot was observed in the isolated single microdroplet due to the absence of any lateral communication (**Figure 11**B). In groups of two or more microdroplets, it was surprising that the reflection-related interactions were found between neighboring microdroplets (Figure 11C–F). When the microdroplets are densely packed into the hexagonally symmetric monolayer, the circular "lit fire-cracker" patterns were formed because of the photonic cross-communication in the neighbor microdroplets (Figure 11G). Morevoer, the intensity of photonic cross-interaction was found to depend strongly on the distance between the microdroplets, and the photonic cross-communication completely disappeared when the distance was five-times larger than the diameter of microdroplets. It is worth mentioning that omnidirectional red-green-blue reflections in the microdroplets has been achived by using a novel thermally stable photosensitive chiral molecular switch (Figure 11A).[124,125] We can also readily modulate the reflection color of every single microdroplets independently, and Figure 11H,I illustrate the "flower-opening" patterns with light-directed iridescent colors in eight monodisperse mocrodroplets. Such monodisperse microdroplets and their periodic arrays would not only provide a rich and fascinating platform for fundamental theoretical studies of micro/nanophotonics with geometric confinements but also hold great potential for applications in the photonic and opto-electronic devices where circularly polarized light with tailored wavelength is preferred.[126,127] For future research, the photonic cross-communication deserves to be futher investigated by incorporating different types of stimuli-sensitive LCs into the microdroplets, and it should be very rewarding work to explore the relationship between the photonic cross-communication properties and the various external factors such as the physical parameters of different liquid-crystalline materials, the configurations of the microdroplets, the presence of different stimuli, and even the dispersion of different functional nanomaterials, e.g., nanoparticles, nanorods, carbon nanotubes, and graphene derivatives.

3.4. Self-Organized 3D Cholesteric Liquid-Crystalline Microshells

Microfluidic techniques have also been demonstrated to fabricate the CLC microshells with spherical configurations that can act as 3D omnidirectional lasers due to the radial molecular arrangement within the cholesteric microshells. Uchida et al. first reported the fabrication of cholesteric microshells with water-oil-water double phase using the microfluidic method,[128]

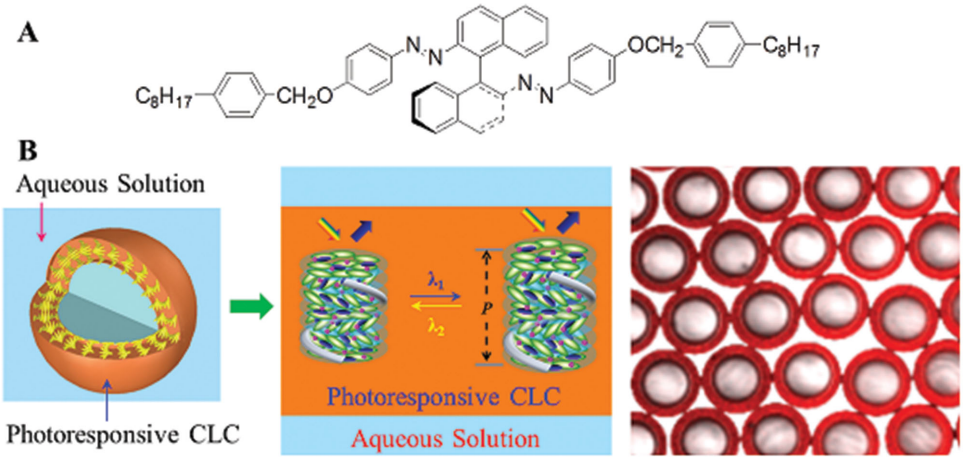

Figure 12. Optically tunable omnidirectional laser in the 3D cholesteric liquid crystalline microshells. A) Molecular structure of light-driven chiral switch. B) (left) Schematic illustrations of the cholesteric microshell and the mechanism of phototunable lasing; (right) Confocal image of the microshells. Reproduced with permission.[129]

in which the oil phase is composed of dye-doped CLCs. By combining different laser-dyes with CLC hosts, three types of laser modes, i.e., distributed feedback (DFB), distributed Bragg reflection (DBF) and WGM resonators, are successfully obtained on the basis of the CLC microshells. Subsequently, Li et al. demonstrated the fabrication and lasing properties of photoresponsive monodisperse cholesteric liquid-crystalline microshells through the capillary-based microfluidic techniques (**Figure 12**),[129] where the photoresponsive CLCs were developed by loading an unprecedented chiral molecular switch responsive to visible light into a nematic liquid-crystalline host. When the cholesteric microshells loaded with DCM laser dye, i.e., (4-(dicyanomethylene)-2-methyl-6-(4-dimethylaminostyryl)-4*H*-pyran), were pumped under an external pulsed laser, the laser emissions in all optical directions were achieved, where the emission wavelength was found to be able to self-tune because of the photoisomerization of azobenezene chiral switch.

The development of self-organized liquid-crystalline microshells is just beginning to be explored, and infinite golden opportunities with numerous challenges may be still hidden in research. It is of paramount importance to endow the monodisperse microshells with versatile functionalities by combining with different novel techniques, e.g., optofluidics and microfluidics. Introduction of various LCs and stimuli in the microshells would further open an attractive avenue for their photonic applications. Additionally, different hydrophilic or hydrophobic laser dyes can be dispersed in the core or microshell parts; in this way it is possible to realize the omnidirectional red–green–blue emissions from one individual microshell. More interestingly, the recent significant advances in the microfluidic technique have enabled us to fabricate a diverse range of novel spherical nanostructures including Janus, core-shell, multicore-shell, and even core-multishell structured geometries.[130,131] The increase in the structural and functional diversity of 3D self-organized microshells would definitely pave a fabulous avenue for their applications in areas of advanced optoelectronic or photonic materials and devices.

4. Self-Organized 3D Topological Defects in Smectic Focal Conic Domains

4.1. Focal Conic Domains in Smectic Liquid Crstals

Recently, self-organized smectic liquid-crystalline materials have received increasing attentions in areas of nanoscience and nanotechnology.[132–134] Among different smectic phases, smectic-A (SmA) phase is the most extensively investigated one, in which focal conic domains (FCDs) are often formed and able to self-organize into a variety of highly periodic 3D nanostructures. Under the planar surface alignment conditions, FCDs spontaneously tend to form highly ordered arrays with hexagonal symmetry, i.e., toric focal conic domains (TFCDs). The fabrication method of these 3D arrays is pretty simple, and perfect TFCD domain arrays can be rapidly generated over a large area just by cooling the smectic LCs from the isotropic state to SmA phase under a planar anchoring condition (**Figure 13**A). The periodic toroid-shaped holes in the 3D nanostructured TFCDs can function as microlenses for focusing the illuminated light due to their intrinsic 3D molecular orientations, while the flat regions between the holes can work as clear windows that allow the light to be directly transmitted as shown in Figure 13B,C.[135] It is worth mentioning that the LC molecular orientation in the TFCD nanostructures can be readily controlled by various stimuli, and therefore it is possible to tune their optical properties by intelligently altering their topologies and internal nanostructures of topological defects.[136,137]

Kim et al. developed a fascinating technique of photolithography by using the 3D TFCD array microlenses as an optically selective photomask, where the novel microstructures could be generated on a photoresist film when the ultraviolet light was illuminated through the TFCD photomask.[138] Interestingly, when the isotropic oscillated illumination light was applied for the photolithography (**Figure 14**A,C), the resultant photoresist patterns were also of isotropic circular shape. However, a fan-shaped nanostructure with two-fold symmetry was unexpectedly generated on the photoresist film (Figure 14B,D), when the polarized illumination light was exploited. In other

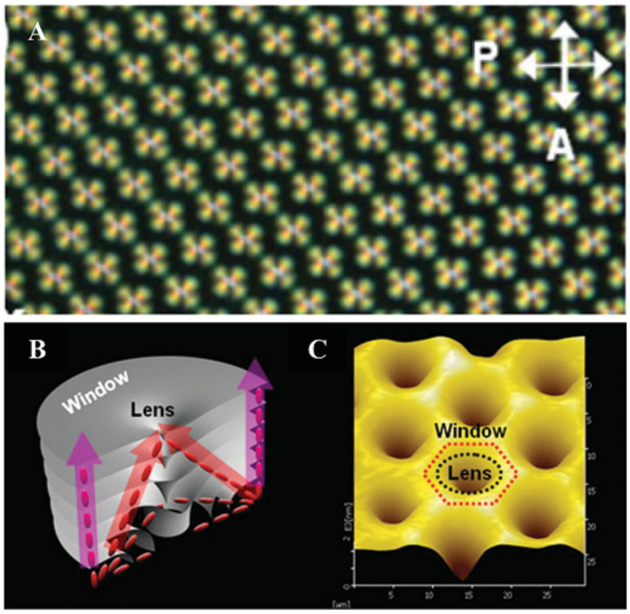

Figure 13. The structures of hexagonally ordered TFCD arrays acting as microlenses. A) The texture of TFCD defect arrays under polarizing optical microscope with crossed polarizers. B) Schematic illustration of a TFCD microlens for focusing incident light. C) Topography image of the TFCD arrays under atomic force microscopy (AFM). Reprinted with permission.[135]

words, the 3D TFCD periodic microlenses can selectively block or pass the incident illumination light by changing the light polarization direction. The concept demonstrated may allow us to fabricate various nano/microscale patterns with tunable sizes, symmetries and geometries just by altering the size of the TFCD, illumination intensity, and the polarization direction of light source. Moreover, the integration of unique nanomaterials within the liquid-crystalline template of 3D topological defects should enable us to fabricate the even more complex hierarchical nanostructures and photonic devices for versatile applications.

4.2. Directing 3D Topological Defects in Smectic Liquid Crystals

Controlling the formation of 3D topological defects in self-organized soft materials is of crucial importance in the development of advanced functional materials and devices, from next-generation ultrafast displays to passive biochemical sensors and beyond.[24] Due to non-covalent and reversible molecular interactions in the liquid-crystalline materials, self-organized 3D topological defects in TFCDs can be expediently regulated by suitably altering the film thickness, anchoring conditions, elastic properties of smectic LCs, etc. Recently, it was reported that diverse shaped TFCDs could be developed by controlling the liquid crystal film thickness on the planar-aligned silicon wafer.[139] As shown in **Figure 15**, perfect TFCD domain arrays can be observed when the thickness of smectic films is in the range of 5 μm > t > 3 μm. Dome-like nanostructures appeared in the TFCDs when the film thickness is in the range of 3 μm > t > 2 μm. In contrast, the liquid-crystalline nanostructures with multiple concentric rings were observed in a much thinner film of t < 2 μm. these kinds of self-organized 3D topological defect domains with adjustable dimensions are highly promising for developing the environment-sensitive superhydrophobic or self-cleaning surfaces like those found in butterfly wings and lotus leaves.

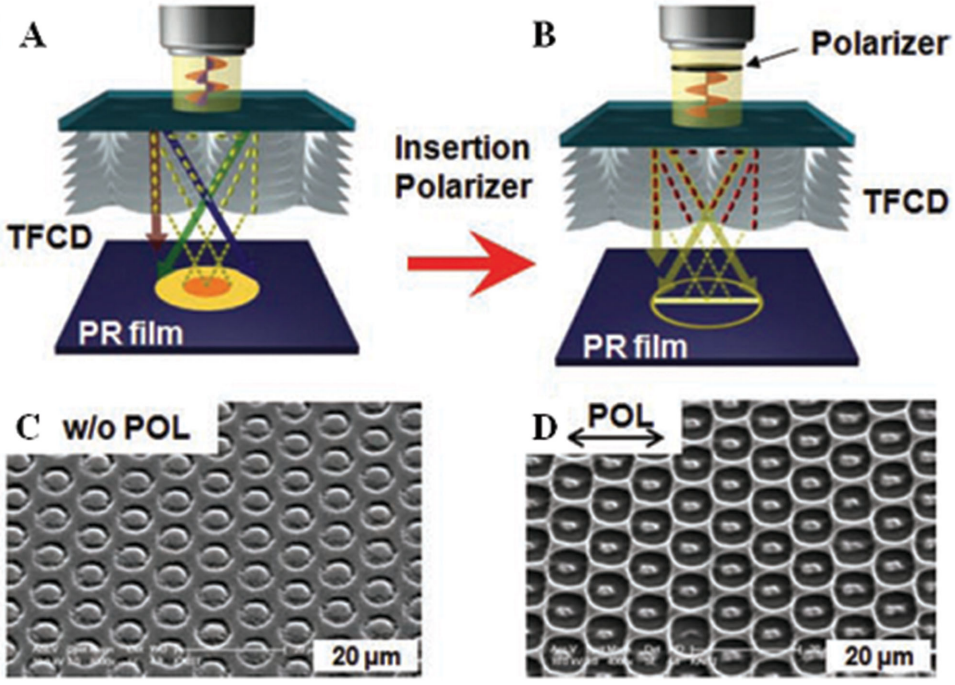

Figure 14. Photolithography using the 3D TFCD arrays as a selectively optical photomask. Schematic presentation of the soft photolithography using A,C) unpolarized and B,D) polarized illumination light, with the corresponding SEM images. Reprinted with permission.[138]

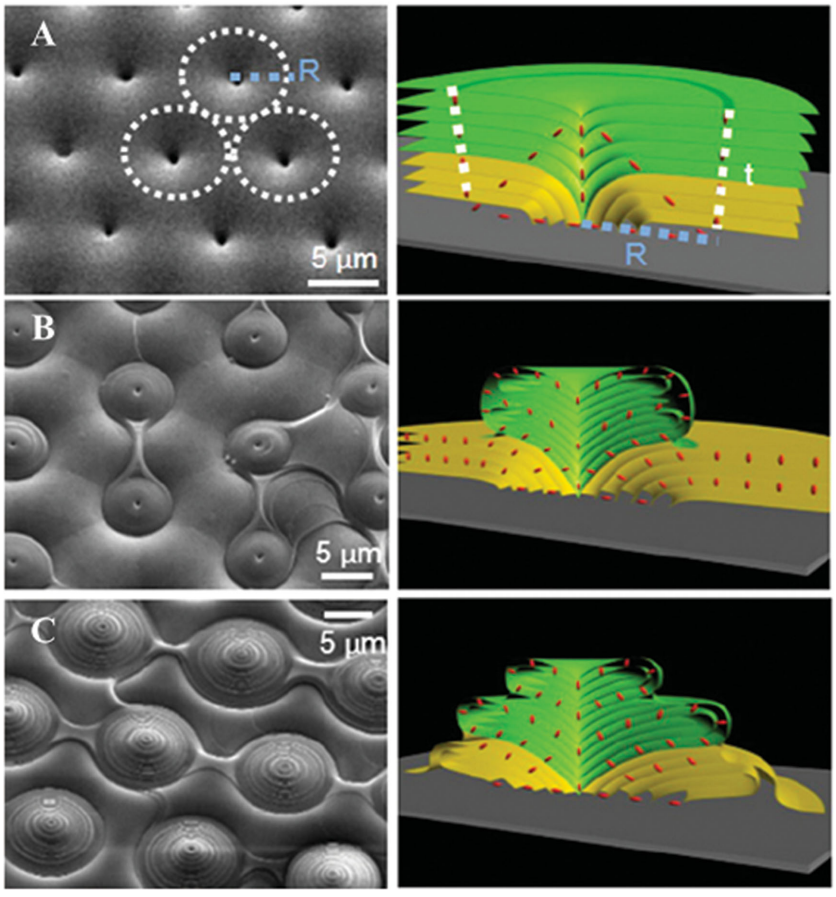

Figure 15. Controllable 3D TFCDs with different LC film thickness (t). SEM images and the corresponding schematic structures of TFCDs on the planar-aligned Si wafer: A) 5 μm > t > 3 μm, B) 3 μm > t > 2 μm, C) t < 2 μm. The radius R of TFCDs is ≈5 μm and t is the thickness of the LC films. Reproduced with permission.[139] Copyright 2013, National Academy of Sciences.

Yang et al. systematically investigated the control over the 3D topological deffects in TFCDs by using the polymer micropillars as a 3D spatially topographic confinement, where the growth of each TFCD domain can be directed by adjusting both the thickness of liquid-crystalline films and the pillar dimensions.[140] It was found that the 3D nature of pillar arrays determined the final topological defect 3D nanostructures within the TFCD arrays, and individual TFCD could be directly grown either in between the neighboring pillars or on top of each pillar as shown in **Figure 16**. This kind of pillar-directed epitaxial assembly is also found to help the conservation between square and hexagonal symmetry of TFCD arrays at a high LC film thickness, and this versatile method may have greater potential to fabricate the periodic TFCD arrays with arbitrary symmetries. The study undoubtedly provides an important guidance for directing self-assembly of 3D topological defects in TFCDs as well as future design and fabrication of the corresponding 3D templates. With further exploration on the corresponding stimuli-responsive properties, this epitaxial approach may open a promising path for novel applications of stimuli-responsive 3D topological defect arrays in areas of tunable lithographic templates and advanced optical and electronic devices.[141]

If the hybrid boundary or anchoring conditions with both planar and homeotropic allignments are applied for directing

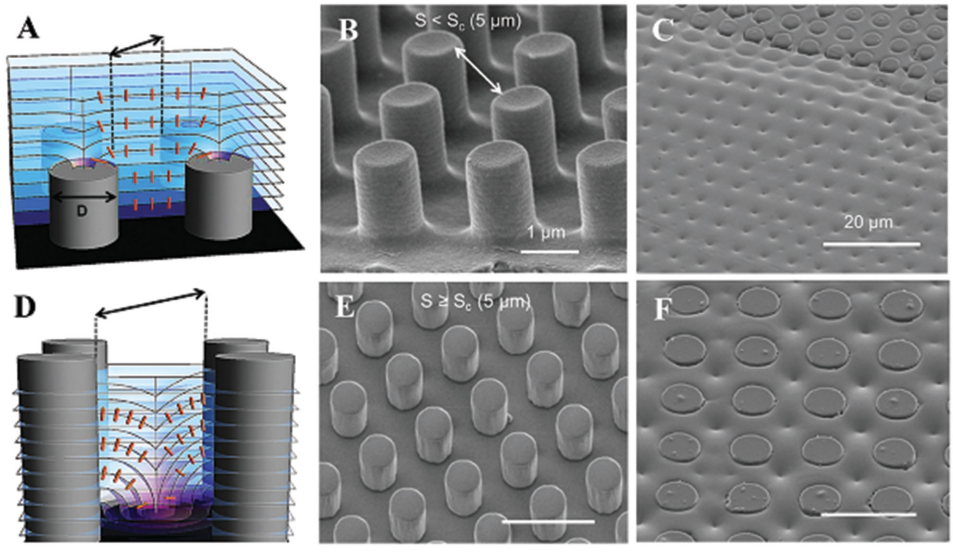

Figure 16. Pillar-assisted epitaxial assembly of 3D TFCDs. Schematic illustrations of SmA LCs confined by a square pillar array where TFCDs were grown either A–C) on top of pillars, or D–F) in between 4 neighboring pillars, with and corresponding SEM images. Reproduced with permission.[140]

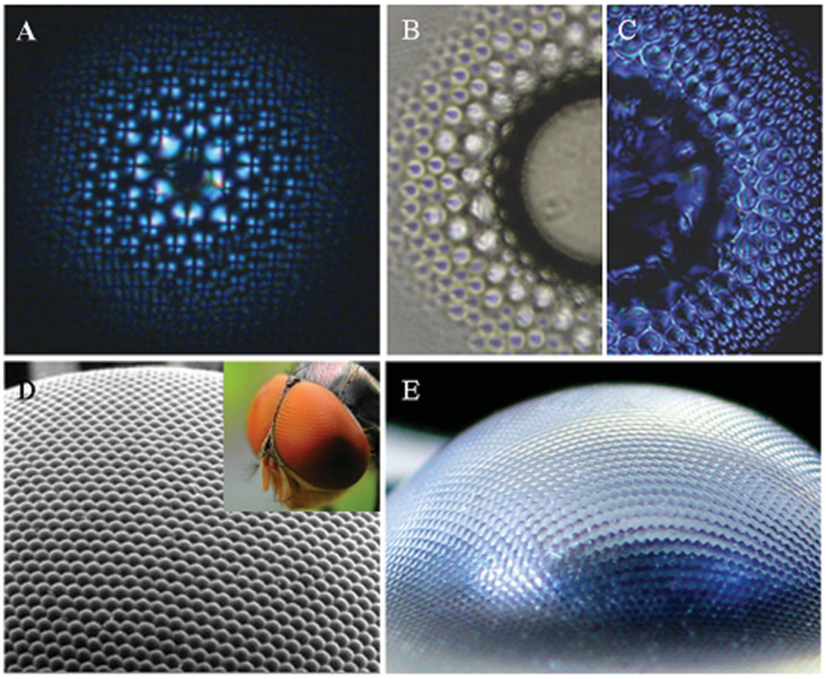

Figure 17. Flower-like 3D self-organized hierarchical nanostructures for "compound eye" microlenses. A) Flower pattern of smectic FCDs generated around a single colloidal particle. Reproduced with permission.[143] Copyright 2013, American Physical Society. Reconfigurable "compound eye" microlenses based on smectic FCDs: B) bright field, C) polarizing optical microscopy. Reproduced with permission.[144] D) Natural and E) artificial compound eyes. Reproduced with permission.[146] Copyright 2012, Optical Society of America.

the self-assembly of FCDs in smectic LCs, novel hierarchical 3D nanostructures with unique functionalities might also be achieved in a single liquid-crystalline thin film.[142] Kamien et al. demonstrated the flower-like self-organization of smectic FCDs (**Figure 17**A), where the hybrid boundary conditions were achieved by combining the curved interfaces of colloidal particles and the topographical alignment of substrates. The hierarchical 3D arrays in the flower pattern are very similar to the so called "compound eyes" in the insects' eyes, which are known to be composed of hundreds of microlenses and able to focus and construct the 3D images (Figure 17D). Recently, Stebe et al. successfully fabricated reconfigurable "compound eye" microlenses composed of well-defined smectic FCDs by using the surface curvature in the micropillar, as shown in Figure 17B–C.[144] From the edge of the micropillar, the size and shape of smectic FCDs varied with a radial distance, which leads to a stepwise change in the focal length of every single flower microlens. It was also found that this kind of self-organized "compound eye" microlenses featured with a wide depth of field and could be reversibly switched or reconfigured under the external stimuli including heating, cooling and light polarization. Compared to the conventional "compound eye" microlenses fabricated by expensive, time-consuming, and scale-prohibitive manufacturing procedures of top-down fabrication techniques (Figure 17E),[145,148] the unique self-organization and other promising attributes in these smectic FCDs make it a quite advantageous approach toward practical applications with a bright future.

For future directions of research, 3D topological defects within the smectic superstructures are also expected to function as tunable templates for directing the dynamically programmable self-assembly of different technologically important nanomaterials, such as functional nanoparticles, nanoplatelets, nanorods, nanotubes, and graphene derivatives, where these dispersed nanobuilding blocks are supposed to self-organize into well-defined functional superstructures with preferred orientations in multiple dimensions. Some nanomaterials, such as silica nanoparticles,[134] gold nanoparticles and carbon nanotubes,[149–151] have so far enjoyed the unprecedented advantages of these 3D smectic nanostructures, but much better golden opportunities may be still in store for other nanomaterials.

5. Self-Organized 3D Polymeric Liquid-Crystalline Nanostructures

Photolithography using multi-beam interference has recently received increasing attention as one of the attractive candidates for fabricating the 3D polymeric photonic nanostructures.[152] The interference photolithography enables a precise and effective control over the size and shape of the resultant nanostructures, and a multitude of novel nano/microsized lattices can be fabricated through the appropriate arrangement and combination of pumped laser beams. Interestingly, the technology has enabled the in situ fast one-step fabrication of stimuli-tunable self-organized 3D polymeric liquid-crystalline photonic nanostructures, i.e., 3D holographic polymer-dispersed LCs (H-PDLCs). Upon exposure to multiple interference laser beams, liquid-crystalline molecules are efficiently trapped into the microdroplets within a polymer network matrix because of the rapid phase separation and polymerization; therefore the periodic nanostructures or patterns with LC-rich or polymer-rich regions can be generated within a few nanoseconds to seconds. The marriage of holography and self-organized LC materials is highly expected to produce a diverse range of novel 3D nanostructures for various applications in electro-optical filters, wavelength division multiplexer, free-space optical switches, information display devices, etc.

To fabricate face-centered-cubic (FCC) nanostructures, a Nd:YAG diode laser emission was split into four beams with equal-intensity and then they were illuminated or exposured upon the liquid-crystalline sample with photopolymerizable monomers in a desired manner (**Figure 18**A–C).[153] Sutherland et al. exploited six beams generated from two continuous-wave lasers for creating an orthorhombic P crystal, i.e., a frequency-doubled, diode pumped Nd:Y-vanadate laser at 532 nm and an Ar-ion laser at 514 nm (Figure 17D–F).[154] Subsequently, diamond-like FCC lattices, which can be operated in the near infrared regions with deeper stopbands, have also

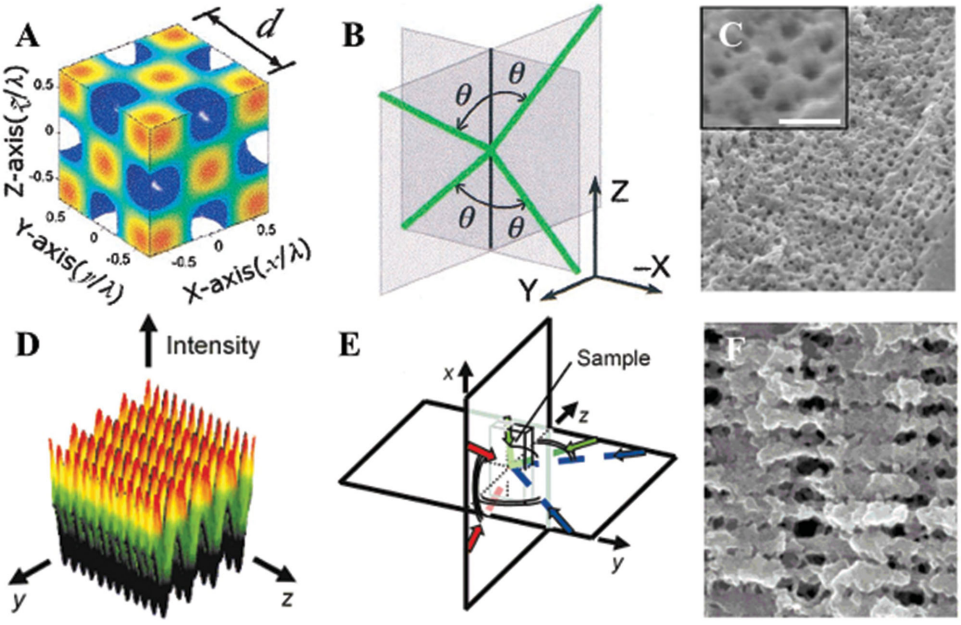

Figure 18. Fabrication of 3D polymeric liquid crystalline nanostructures**.** A–C: Calculated isointensity surface, laser beam geometry and SEM images in H-PDLC with FCC lattice. Reproduced with permission.[153] Copyright 2003, Optical Society of America. D–F) Calculated isointensity surface, laser beam geometry and SEM images in H-PDLC with orthorhombic P lattice. Reproduced with permission.[154]

been fabricated by using four polarized coherent beams of a 532 nm diode laser.[155] Importantly, the diffractive properties of these 3D photonic nanostructures can be readily tuned by controlling the LC molecular orientation with various stimuli including heat, stress, electric and magnetic field, etc.[156] Given the contemporary significance of photolithography technique, it can be anticipated that the combination of unique liquid-crystalline materials with the promising self-assembly processes using multi-beam interference might lead to outstanding and unprecedented photonic nanomaterials and devices for all kinds of potential applications such as high density data storage, stimuli sensors, and micro/nanophotonics.

6. Conclusions and Perspectives

In this review, we furnished a glimpse of the research advancements in design, fabrication and applications of stimuli-directing self-organized 3D liquid-crystalline photonic nanostructures, including self-organized 3D cubic BP nanostructures, self-organized 3D liquid-crystalline microdroplets and microshells, 3D topological defects in smectic focal conic domains, and 3D polymeric liquid-crystalline nanostructures. Due to their unique self-organized properties and ultrasensitivity to different external perturbations or stimuli, these nanostructures can efficiently and selectively transmit and amplify local information or properties in a controllable and even programmable manner from molecular levels to macroscopic scales, thus opening an attractive route for versatile advanced photonic applications. These liquid-crystalline nanostructures are also expected to function as powerful soft templates to direct the dynamic self-assembly of nanomaterials into various well-defined functional architectures via different non-covalent molecular interactions over multiple length scales, which would offer new opportunities for the development of fundamental science and their emerging applications. Furthermore, it would be of great interest to develop the liquid-crystalline 3D photonic nanostructures directly from anisotropic nanoparticles and their mixtures in the future research.[157] The unique and intrinsic optical, mechanical, electrical and magnetic properties of these anisotropic building blocks will endow the resultant materials and photonic devices with superior performance.[158–161] Owing to their preferred orientation and ordering, these anisotropic nanoparticles themselves could self-organize into functional 3D hierarchical architectures with unprecedented properties, via processing from their liquid-crystalline phases.[162,163]

It is anticipated that these liquid crystalline materials would play an increasingly important role in the prosperous area of nanoscience and nanotechnology, and such a promising research field would also give rise to meaningful multidisciplinary cooperation of scientists and engineers from different backgrounds. Nature is a fabulous gallery of various complex photonic nanostructures which have been formed through evolution and natural selection over billions of years. All living creatures in nature are composed mostly of soft matter with extraordinary complexity and high efficiency, where the discrete building blocks are self-assembled via complex and multiple interactions. From this point of view, photonic crystals or nanostructures using liquid-crystalline materials are supposed to open a brand new door for soft matter photonics with an exciting future, where bottom-up self-assembly approaches are expected to enable the cost-effective, environment-friendly and large scale production of various fabulous soft superstructures with a number of unrivalled properties, such as multi-stimuli-responsiveness, easy tunability, and real time reconfigurability. However, related research in this field is still in a preliminary

stage, and future investigation in such promising topics with infinite possibilities would not only broaden our knowledge of soft photonics but also promote their diverse applications as intelligent advanced functional materials.

Acknowledgements

Financial support by the AFOSR (FA9950–09–1–0193 and FA9950–09–1–0254) (molecular motor and gold nanorod studies), the U.S. Department of Energy, Office of Science, Office of Basic Energy Sciences (Grant DE-SC0001412) (bent-core intermediate and mesogen studies), the DoD-MURI (FA9550–12–1–0037) (3D architecture studies), and the DoD-Army (laser protection studies), NASA (near-to-mid IR sensor studies) is gratefully acknowledged. We thank all the Li's lab current and former members as well as his collaborators, whose names can be found in the references, for their significant contributions in this project.

Received: May 19, 2015
Revised: August 4, 2015
Published online: November 9, 2015

[1] J. H. Moon, S. Yang, *Chem. Rev.* **2009**, *110*, 547.
[2] *Intelligent Stimuli-Responsive Materials: From Well-Defined Nanostructures to Applications* (Ed: Q. Li), John Wiley & Sons, Hoboken, NJ, USA **2013**.
[3] A. R. Parker, V. L. Welch, D. Driver, N. Martini, *Nature* **2003**, *426*, 786.
[4] Y. Zhao, Z. Xie, H. Gu, C. Zhu, Z. Gu, *Chem. Soc. Rev.* **2012**, *41*, 3297.
[5] P. Vukusic, J. R. Sambles, *Nature* **2003**, *424*, 852.
[6] P. Vukusic, *Phys. World* **2004**, *17*, 35.
[7] V. Saranathan, C. O. Osuji, S. Mochrie, H. Noh, S. Narayanan, A. Sandy, E. R. Dufresne, R. O. Prum, *Proc. Natl. Acad. Sci. USA* **2010**, *107*, 11676.
[8] V. Welch, V. Lousse, O. Deparis, A. Parker, J. P. Vigneron, *Phys. Rev. E* **2007**, *75*, 041919.
[9] J. Aizenberg, A. Tkachenko, S. Weiner, L. Addadi, G. Hendler, *Nature* **2001**, *412*, 819.
[10] J. Aizenberg, D. A. Muller, J. L. Grazul, D. R. Hamann, *Science* **2003**, *299*, 1205.
[11] J. Aizenberg, G. Hendler, *J. Mater. Chem.* **2004**, *14*, 2066.
[12] Y. Xia, B. Gates, Z. Y. Li, *Adv. Mater.* **2001**, *13*, 409.
[13] G. A. Ozin, S. M. Yang, *Adv. Funct. Mater.* **2001**, *11*, 95.
[14] A. C. Edrington, A. M. Urbas, P. DeRege, C. X. Chen, T. M. Swager, N. Hadjichristidis, M. Xenidou, L. J. Fetters, J. D. Joannopoulos, Y. Fink, E. L. Thomas, *Adv. Mater.* **2001**, *13*, 421.
[15] J. H. Lee, Y. S. Kim, K. Constant, K. M. Ho, *Adv. Mater.* **2007**, *19*, 791.
[16] G. M. Gratson, F. Garcia-Santamaria, V. Lousse, M. J. Xu, S. H. Fan, J. A. Lewis, P. V. Braun, *Adv. Mater.* **2006**, *18*, 461.
[17] J. H. Kang, J. H. Moon, S. K. Lee, S. G. Park, S. G. Jang, S. Yang, S. M. Yang, *Adv. Mater.* **2008**, *20*, 3061.
[18] J. H. Jang, S. J. Jhaveri, B. Rasin, C. Koh, C. K. Ober, E. L. Thomas, *Nano Lett.* **2008**, *8*, 1456.
[19] J. Ge, Y. Yin, *Angew. Chem. Int. Ed.* **2011**, *50*, 1492.
[20] M. Honda, T. Seki, Y. Takeoka, *Adv. Mater.* **2009**, *21*, 18014.
[21] I. W. Hamley, *Angew. Chem. Int. Ed.* **2003**, *42*, 1692.
[22] J. Y. Cheng, C. A. Ross, H. I. Smith, E. L. Thomas, *Adv. Mater.* **2006**, *19*, 2505.
[23] M. R. Bockstaller, R. A. Mickiewicz, E. L. Thomas, *Adv. Mater.* **2005**, *17*, 1331.
[24] *Nanoscience with Liquid Crystals: From Self-Organized Nanostructures to Applications* (Ed: Q. Li), Springer, Heidelberg, Germany **2014**.
[25] Y. Wang, Q. Li, *Adv. Mater.* **2012**, *24*, 1926.
[26] Q. Li, Y. Li, J. Ma, D.-K. Yang, T. J. White, T. J. Bunning, *Adv. Mater.* **2011**, *23*, 5069.
[27] Y. Li, M. Wang, T. J. White, T. J. Bunning, Q. Li, *Angew. Chem. Int. Ed.* **2013**, *52*, 8925.
[28] M. Mathews, R. Zola, S. Hurley, D. Yang, T. J. White, T. J. Bunning, Q. Li, *J. Am. Chem. Soc.* **2010**, *132*, 18361.
[29] H. K. Bisoyi, Q. Li, *Liquid Crystals in Kirk-Othmer Encyclopedia of Chemical Technology*, John Wiley & Sons, Honoken, NJ, USA **2014**.
[30] *Liquid Crystals Beyond Displays: Chemistry, Physics, and Applications* (Ed: Q. Li), John Wiley and Sons, Hoboken, NJ, USA **2012**.
[31] L. Wang, Q. Li, in *Organic & Hybrid Photonic Crystals*, (Ed: D. Comoretto), Springer, New York, NY, USA **2015**, Ch. 18.
[32] H. K. Bisoyi, Q. Li, *Acc. Chem. Res.* **2014**, *47*, 3184.
[33] D. C. Wright, N. D. Mermin, *Rev. Modern Phys.* **1989**, *61*, 385.
[34] F. Castles, S. M. Morris, E. M. Terentjev, H. J. Coles, *Phys. Rev. Lett.* **2010**, *104*, 157801.
[35] H. Kikuchi, *Struct. Bonding* **2008**, *128*, 99.
[36] L. Wang, W. He, X. Xiao, F. Meng, Y. Zhang, P. Yang, L. Wang, H. Yang, *Small* **2012**, *8*, 2189.
[37] Y. Hisakado, H. Kikuchi, T. Nagamura, T. Kajiyama, *Adv. Mater.* **2005**, *17*, 96.
[38] Y. Haseba, H. Kikuchi, T. Nagamura, T. Kajiyama, *Adv. Mater.* **2005**, *17*, 2311.
[39] L. Wang, W. He, X. Xiao, Q. Yang, B. Li, P. Yang, H. Yang, *J. Mater. Chem.* **2012**, *22*, 2383.
[40] L. Wang, W. He, M. Wang, M. Wei, J. Sun, X. Chen, H. Yang, *Liq. Cryst.* **2013**, *40*, 354.
[41] B. Li, W. He, L. Wang, X. Xiao, H. Yang, *Soft Matter* **2013**, *9*, 1172.
[42] L. Wang, L. Yu, X. Xiao, Z. Wang, P. Yang, W. He, H. Yang, *Liq. Cryst.* **2012**, *39*, 629.
[43] P. Etchegoin, *Phys. Rev. E* **2000**, *62*, 1435.
[44] R. M. Hornreich, S. Shtrikman, *Phys. Lett.* **1981**, *82A*, 345.
[45] W. Cao, A. Muñoz, P. Palffy-Muhoray, B. Taheri, *Nat. Mater.* **2002**, *1*, 111.
[46] H. Coles, S. Morris, *Nature Photonics* **2010**, *4*, 676.
[47] H. S. Sözüer, J. P. Dowling, *J. Mod. Optic.* **1994**, *41*, 231.
[48] H. S. Sözüer, J. W. Haus, *J. Opt. Soc. Am. B* **1993**, *10*, 296.
[49] S. Yokoyama, S. Mashiko, H. Kikuchi, K. Uchida, T. Nagamura, *Adv. Mater.* **2006**, *18*, 48.
[50] S. Morris, A. Ford, C. Gillespie, M. Pivnenko, O. Hadeler, H. J. Coles, *J. Soc. Inf. Display* **2006**, *14*, 565.
[51] C.-W. Chen, H.-C. Jau, C.-T. Wang, C.-H. Lee, I. C. Khoo, T.-H. Lin, *Opt. Express* **2012**, *20*, 23978.
[52] H. Choi, H. Higuchi, H. Kikuchi, *Soft Matter* **2011**, *7*, 4252.
[53] S. T. Hur, B. R. Lee, M. J. Gim, K.W. Park, M. H. Song, S. W. Choi, *Adv. Mater.* **2013**, *21*, 3002.
[54] K. Kim, S. T. Hur, S. Kim, S. Y. Jo, B. R. Lee, M. H. Song, S.-W. Choi, *J. Mater. Chem. C* **2015**, *3*, 5383.
[55] P. Pollmann, E. Voss, *Liq. Cryst.* **1997**, *23*, 299.
[56] F. Castles, S. M. Morris, J. M. C. Hung, M. M. Qasim, A. D. Wright, S. Nosheen, S. S. Choi, B. I. Outram, S. J. Elston, C. Burgess, L. Hill, T. D. Wilkinson, H. J. Coles, *Nat. Mater.* **2014**, *13*, 817.
[57] H. Finkelmann, S. T. Kim, A. Muñoz, P. Palffy-Muhoray, B. Taheri, *Adv. Mater.* **2011**, *13*, 1069.
[58] P. P. Crooker, in *Chirality in Liquid Crystals* (Eds: H.-S. Kitzerow, C. Bahr), Springer-Verlag, New York, NY, USA **2001**, Ch. 7.
[59] J. Yan, L. Rao, M. Jiao, H. C. Cheng, S. T. Wu, *J. Mater. Chem.* **2011**, *21*, 7870.
[60] G. Heppke, M. Krumrey, F. Oestreicher, *Mol. Cryst. Liq. Cryst.* **1983**, *99*, 99.

[61] H. J. Coles, M. N. Pivnenko, *Nature* **2005**, *436*, 997.
[62] S.-Y. Lu, L.-C. Chien, *Opt. Lett.* **2010**, *35*, 562.
[63] A. Chanishvili, G. Chilaya, G. Petriashvili, P. J. Collings, *Phys. Rev. E* **2005**, *71*, 051705.
[64] H. Y. Liu, C.-T. Wang, C.-Y. Hsu, T.-H. Lin, J.-H. Liu, *Appl. Phys. Lett.* **2010**, *96*, 121103.
[65] X. Chen, L. Wang, C. Li, J. Xiao, H. Ding, X. Liu, X. Zhang, W. He, H. Yang, *Chem. Commun.* **2013**, *49*, 10097.
[66] T.-H. Lin, Y. Li, C.-T. Wang, H.-C. Jau, C.-W. Chen, C.-C. Li, H. K. Bisoyi, T. J. Bunning, Q. Li, *Adv. Mater.* **2013**, *25*, 5050.
[67] N. Horiuchi, *Nature Photonics* **2013**, *7*, 767.
[68] L. Wang, H. Dong, Y. Li, C. Xue, L.-D. Sun, C.-H. Yan, Q. Li, *J. Am. Chem. Soc.* **2014**, *136*, 4480.
[69] K. G. Gutiérrez-Cuevas, L. Wang, C. Xue, S. Gautam, S. Kumar, A. Urbas, Q. Li, *Chem. Comm.* **2015**, *51*, 9845.
[70] Y. Wang, A. Urbas, Q. Li, *J. Am. Chem. Soc.* **2012**, *134*, 3342.
[71] L. Wang, H. Dong, Y. Li, R. Liu, Y.-F. Wang, H. K. Bisoyi, L.-D. Sun, C.-H. Yan, Q. Li, *Adv. Mater.* **2015**, *27*, 2065.
[72] L. Wang, K. G. Gutierrez-Cuevas, A. Urbas, Q. Li, unpublished.
[73] H. Coles, M. Pivnenko, *Nature* **2005**, *436*, 997.
[74] H. Kikuchi, M. Yokota, Y. Hisakado, H. Yang, T. Kajikawa, *Nat. Mater.* **2002**, *1*, 64.
[75] H. Lee, H. J. Park, O. J. Kwon, S. J. Yun, J. H. Park, S. Hong, S. T. Shin, *SID Symposium Digest.* **2011**, *42*, 121.
[76] Y. Han, K. Pacheco, C. W. Bastiaansen, D. J. Broer, R. P. Sijbesma, *J. Am. Chem. Soc.* **2010**, *132*, 2961.
[77] A. Saha, Y. Tanaka, Y. Han, C. M. W. Bastiaansen, D. J. Broer, R. P. Sijbesm, *Chem. Commun.* **2012**, *48*, 4579.
[78] X. Su, S. Voskian, R. P. Hughes, I. Aprahamian, *Angew. Chem. Int. Ed.* **2013**, *52*, 10934.
[79] N. Herzer, H. Guneysu, D. J. D. Davies, D. Yildirim, A. R. Vaccaro, D. J. Broer, C. W. M. Bastiaansen, A. P. H. J. Schenning, *J. Am. Chem. Soc.* **2012**, *134*, 7608.
[80] P. V. Shibaev, K. Schaumburg, V. Plaksin, *Chem. Mater.* **2002**, *14*, 959.
[81] P. V. Shibaev, R. L. Sanford, D. Chiappetta, P. Rivera, *Mol. Cryst. Liq. Cryst.* **2007**, *479*, 161.
[82] P. V. Shibaev, D. Chiappetta, R. L. Sanford, P. Palffy-Muhoray, M. Moreira, W. Cao, M. M. Green, *Macromolecules* **2006**, *39*, 3986.
[83] C.-K. Chang, C. M. W. Bastiaansen, D. J. Broer, H.-L. Kuo, *Adv. Funct. Mater.* **2012**, *22*, 2855.
[84] D. J. Mulder, A. P. H. J. Schenning, C. W. M. Bastiaansen, *J. Mater. Chem. C* **2014**, *2*, 6695.
[85] I. B. Burgess, M. Lončar, J. Aizenberg, *J. Mater. Chem. C* **2013**, *1*, 6075.
[86] K. Stratford, O. Henrich, J. S. Lintuvuori, M. E. Cates, D. Marenduzzo, *Nat. Comm.* **2014**, *5*, 3594.
[87] L. Wang, W. He, X. Xiao, M. Wang, M. Wang, P. Yang, Z. Zhou, H. Yang, H. Yu, Y. Lu, *J. Mater. Chem.* **2012**, *22*, 19629.
[88] L. Wang, W. He, Q. Wang, M. Yu, X. Xiao, Y. Zhang, M. Ellahi, Z. Yang, D. Zhao, H. Yang, L. Guo, *J. Mater. Chem. C* **2013**, *1*, 6526.
[89] M. Ravnik, G. P. Alexander, J. M. Yeomans, S. Žumer, *Proc. Nat. Acad. Sci. USA* **2011**, *108*, 5188.
[90] O. D. Lavrentovich, *Proc. Natl Acad. Sci. USA* **2011**, *108*, 5143.
[91] F. Castles, F. V. Day, S. M. Morris, D.-H. Ko, D. J. Gardiner, M. M. Qasim, S. Nosheen, P. Hands, S. S. Choi, R. H. Friend, H. J. Coles, *Nat. Mater.* **2012**, *11*, 599.
[92] G. Cipparrone, A. Mazzulla, A. Pane, R. J. Hernandez, R. Bartolino, *Adv. Mater.* **2011**, *23*, 5773.
[93] R. J. Hernández, *Ph.D. Thesis*, University of Calabria, Italy, **2012**.
[94] P. S. Drzaic, *Liquid Crystal Dispersions*, World Scientific, Singapore, **1995**.
[95] F. C. Mackintosh, T. C. Lubensky, *Phys. Rev. Lett.* **1991**, *67*, 1169.
[96] J. H. Erdmann, S. Zumer, J. W. Doane, *Phys. Rev. Lett.* **1990**, *64*, 1907.
[97] P. G. de Gennes, J. Prost, *The Physics of Liquid Crystals*, Oxford University Press, Oxford, **2001**.
[98] F. Xu, P. P. Crooker, *Phys. Rev. E* **1997**, *56*, 6853.
[99] J. K. Gupta, S. Sivakumar, F. Caruso, N. L. Abbott, *Angew. Chem. Int. Ed.* **2009**, *48*, 1652.
[100] I. H. Lin, D. S. Miller, P. J. Bertics, C. J. Murphy, J. J. de Pablo, N. L. Abbott, *Science* **2011**, *332*, 1297.
[101] A. Fernández-Nieves, G. Cristobal, V. Garcés-Chávez, G. C. Spalding, K. Dholakia, D. A. Weitz, *Adv. Mater.* **2005**, *17*, 680.
[102] F. Mondiot, X. Wang, J. J. de Pablo, N. L. Abbott, *J. Am. Chem. Soc.* **2013**, *135*, 9972.
[103] M. Vennes, S. Martin, T. Gisler, R. Zentel, *Macromolecules* **2006**, *39*, 8326.
[104] A. M. Lowe, N. L. Abbott, *Chem. Mater.* **2011**, *24*, 746.
[105] M. Humar, *Ph.D. Thesis*, Jozef Stefan Institute, Ljubljana, Slovenia, **2012**.
[106] J. A. Moreno-Razo, E. J. Sambriski, N. L. Abbott, J. P. Hernández-Ortiz, J. J. De Pablo, *Nature* **2012**, *485*, 86.
[107] D. S. Miller, X. Wang, N. L. Abbott, *Chem. Mater.* **2013**, *26*, 496.
[108] J. W. Doane, N. A. Vaz, B. G. Wu, S. Zumer, *Appl. Phys. Lett.* **1986**, *48*, 269.
[109] M. Humar, M. Ravnik, S. Pajk, I. Muševič, *Nat. Photonics* **2009**, *3*, 595.
[110] A. Ashkin, J. M. Dziedzic, *Phys. Rev. Lett.* **1977**, *38*, 1351.
[111] K. J. Vahala, *Nature* **2003**, *424*, 839.
[112] I. Musevic, M. Skarabo, M. Humar, *J. Phys.: Condens. Matter.* **2011**, *23*, 284112.
[113] I. Musevic, M. Humar, *Proc. SPIE* **2011**, *7955*, 795509.
[114] M. Humar, I. Musevic, *Opt. Express* **2011**, *19*, 19836.
[115] K. G. Sullivan, D. G. Hall, *Phys. Rev. A* **1994**, *50*, 2701.
[116] D. Brady, G. Papen, J. E. Sipe, *J. Opt. Soc. Am. B* **1993**, *10*, 644.
[117] G. N. Burlak, *Phys. Lett. A* **2002**, *299*, 94.
[118] Y. Xu, W. Liang, A. Yariv, J. G. Fleming, S.-Y. Lin, *Opt. Lett.* **2004**, *29*, 424.
[119] A. Tandaechanurat, S. Ishida, K. Aoki, D. Guimard, M. Nomura, S. Iwamoto, Y. Arakawa, *Appl. Phys. Lett.* **2009**, *94*, 171115.
[120] I. Gourevich, L. M. Field, Z. Wei, C. Paquet, A. Petukhova, A. Alteheld, E. Kumacheva, J. J. Saarinen, J. E. Sipe, *Macromolecules* **2006**, *39*, 1449.
[121] M. Humar, I. Musevic, *Opt. Express* **2010**, *18*, 26995.
[122] S. Utada, E. Lorenceau, D. R. Link, P. D. Kaplan, H. A. Stone, D. A. Weitz, *Science* **2005**, *308*, 537.
[123] J. Fan, Y. Li, H. K. Bisoyi, R. S. Zola, D. K. Yang, T. J. Bunning, D. A. Weitz, Q. Li, *Angew. Chem. Int. Ed.* **2015**, *54*, 2160.
[124] Y. Li, C. Xue, M. Wang, A. Urbas, Q. Li, *Angew. Chem. Int. Ed.* **2013**, *52*, 13703.
[125] Y. Li, A. Urbas, Q. Li, *J. Am. Chem. Soc.* **2012**, *134*, 9573.
[126] J. Chen, E. Lacaze, E. Brasselet, S. R. Harutyunyan, N. Katsonis, B. L. Feringa, *J. Mater. Chem. C* **2014**, *2*, 8137.
[127] J. Noh, H. L. Liang, I. Drevensek-Olenik, J. P. F. Lagerwall, *J. Mater. Chem. C* **2014**, *2*, 806.
[128] Y. Uchida, Y. Takanishi, J. Yamamoto, *Adv. Mater.* **2013**, *25*, 3234.
[129] L. Chen, Y. Li, J. Fan, H. K. Bisoyi, D. A. Weitz, Q. Li, *Adv. Opt. Mater.* **2014**, *2*, 845.
[130] Y. Zhao, L. Shang, Y. Cheng, Z. Gu, *Acc. Chem. Res.* **2014**, *47*, 3632.
[131] Y. Zhao, Y. Cheng, L. Shang, J. Wang, Z. Xie, Z. Gu, *Small* **2015**, *11*, 151.
[132] Y. H. Kim, D. K. Yoon, H. S. Jeong, J. H. Kim, E. K. Yoon, H.-T. Jung, *Adv. Func. Mater.* **2009**, *19*, 3008.
[133] A. Honglawan, S. Yang, in *Nanoscience with Liquid Crystals* (Ed: Q. Li), Springer, Heidelberg, Germany **2014**, Ch. 2.
[134] D. K. Yoon, M. C. Choi, Y. H. Kim, M. W. Kim, O. D. Lavrentovich, H.-T. Jung, *Nat. Mater.* **2007**, *6*, 866.
[135] Y. H. Kim, D. K. Yoon, H. S. Jeong, O. D. Lavrentovich, H. T. Jung, *Adv. Funct. Mater.* **2011**, *21*, 610.
[136] M. Kleman, O. D. Lavrentovich, *Liq. Cryst.* **2009**, *36*, 1085.

[137] I. Gryn, E. Lacaze, R. Bartolino, B. Zappone, *Adv. Funct. Mater.* **2015**, *25*, 142.
[138] Y. H. Kim, J. O. Lee, H. S. Jeong, J. H. Kim, E. K. Yoon, D. K. Yoon, J. B. Yoon, H. T. Jung, *Adv. Mater.* **2010**, *22*, 2416.
[139] D. K. Yoon, Y. H. Kim, D. S. Kim, S. D. Oh, I. I. Smalyukh, N. A. Clark, H. T. Jung, *Proc. Nat. Acad. Sci. USA* **2013**, *110*, 19263.
[140] A. Honglawan, D. A. Beller, M. Cavallaro, R. D. Kamien, K. J. Stebe, S. Yang, *Adv. Mater.* **2011**, *23*, 5519.
[141] A. Honglawan, D. A. Beller, M. Cavallaro, R. D. Kamien, K. J. Stebe, S. Yang, *Proc. Nat. Acad. Sci. USA* **2013**, *110*, 34.
[142] C. Meyer, L. L. Cunff, M. Belloul, G. Foyart, *Materials* **2009**, *2*, 499.
[143] D. A. Beller, M. A. Gharbi, A. Honglawan, K. J. Stebe, S. Yang, R. D. Kamien, *Phys. Rev. X* **2013**, *3*, 041026.
[144] F. Serra, M. A. Gharbi, Y. Luo, I. B. Liu, N. D. Bade, R. D. Kamien, S. Yang, K. J. Stebe, *Adv. Opt. Mater.* **2015**, *3*, 1287.
[145] K. H. Jeong, J. Kim, L. P. Lee, *Science* **2006**, *312*, 557.
[146] P. Qu, F. Chen, H. Liu, Q. Yang, J. Lu, J. Si, Y. Wang, X. Hou, *Optics Express* **2012**, *20*, 5775.
[147] Y. M. Song, Y. Xie, V. Malyarchuk, J. Xiao, I. Jung, K. J. Choi, Z. Liu, H. Park, C. Lu, R. H. Kim, R. Li, K. B. Crozier, Y. Huang, J. A. Rogers, *Nature* **2013**, *497*, 95.
[148] L. Dong, A. K. Agarwal, D. J. Beebe, H. Jiang, *Nature* **2006**, *442*, 551.
[149] J. Milette, S. Relaix, C. Lavigne, V. Toader, S. J. Cowling, I. M. Saez, R. B. Lennox, J. W. Goodby, L. Reven, *Soft Matter* **2012**, *8*, 2593.
[150] D. Coursault, J. Grand, B. Zappone, H. Ayeb, G. Lévi, N. Félidj, E. Lacaze, *Adv. Mater.* **2012**, *24*, 1461.
[151] H. S. Jeong, Y. K. Ko, Y. H. Kim, D. K. Yoon, H.-T. Jung, *Carbon* **2010**, *48*, 774.
[152] J. H. Moon, J. Ford, S. Yang, *Polym. Adv. Technol.* **2006**, *17*, 83.
[153] M. J. Escuti, J. Qi, G. P. Crawford, *Opt. Lett.* **2003**, *28*, 522.
[154] V. P. Tondiglia, L. V. Natarajan, R. L. Sutherland, D. Tomlin, T. J. Bunning, *Adv. Mater.* **2002**, *14*, 187.
[155] M. Escuti, G. Crawford, *Mol. Cryst. Liq. Cryst.* **2004**, *421*, 23.
[156] Y. Liu, X. W. Sun, *Adv. OptoElectron.* **2008**, 684349.
[157] H. K. Bisoyi, Q. Li, in *Anisotropic Nanomaterials* (Ed: Q. Li), Springer, Heidelberg, Germany **2015**, Ch. 6.
[158] M. Wang, L. He, S. Zorba, Y. Yin, *Nano Lett.* **2014**, *14*, 3966.
[159] T.-Z. Shen, S.-H. Hong, J.-K. Song, *Nat. Mater.* **2014**, *13*, 394.
[160] Z. Xu, C. Gao, *Nat. Commun.* **2011**, *2*, 571.
[161] H. Ko, V. V. Tsukruk, *Nano Lett.* **2006**, *6*, 1443.
[162] H. P. Cong, J. F. Chen, S. H. Yu, *Chem. Soc. Rev.* **2014**, *43*, 7295.
[163] S. Nardecchia, D. Carriazo, M. L. Ferrer, M. C. Gutierrez, F. del Monte, *Chem. Soc. Rev.* **2013**, *42*, 794.